

Identification of specific sources of airborne particles emitted from within a complex industrial (steelworks) site

Beddows, David; Harrison, Roy

DOI:

[10.1016/j.atmosenv.2018.03.055](https://doi.org/10.1016/j.atmosenv.2018.03.055)

License:

Creative Commons: Attribution-NonCommercial-NoDerivs (CC BY-NC-ND)

Document Version

Peer reviewed version

Citation for published version (Harvard):

Beddows, D & Harrison, R 2018, 'Identification of specific sources of airborne particles emitted from within a complex industrial (steelworks) site', *Atmospheric Environment*, vol. 183, pp. 122-134.

<https://doi.org/10.1016/j.atmosenv.2018.03.055>

[Link to publication on Research at Birmingham portal](#)

Publisher Rights Statement:

Checked for eligibility: 13/04/2018

<https://www.sciencedirect.com/science/article/pii/S1352231018302176>

<https://doi.org/10.1016/j.atmosenv.2018.03.055>

General rights

Unless a licence is specified above, all rights (including copyright and moral rights) in this document are retained by the authors and/or the copyright holders. The express permission of the copyright holder must be obtained for any use of this material other than for purposes permitted by law.

- Users may freely distribute the URL that is used to identify this publication.
- Users may download and/or print one copy of the publication from the University of Birmingham research portal for the purpose of private study or non-commercial research.
- User may use extracts from the document in line with the concept of 'fair dealing' under the Copyright, Designs and Patents Act 1988 (?)
- Users may not further distribute the material nor use it for the purposes of commercial gain.

Where a licence is displayed above, please note the terms and conditions of the licence govern your use of this document.

When citing, please reference the published version.

Take down policy

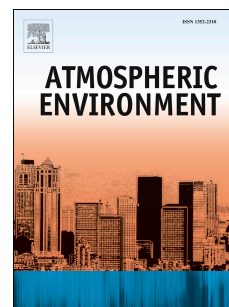
While the University of Birmingham exercises care and attention in making items available there are rare occasions when an item has been uploaded in error or has been deemed to be commercially or otherwise sensitive.

If you believe that this is the case for this document, please contact UBIRA@lists.bham.ac.uk providing details and we will remove access to the work immediately and investigate.

Accepted Manuscript

Identification of specific sources of airborne particles emitted from within a complex industrial (steelworks) site

D.C.S. Beddows, Roy M. Harrison



PII: S1352-2310(18)30217-6

DOI: [10.1016/j.atmosenv.2018.03.055](https://doi.org/10.1016/j.atmosenv.2018.03.055)

Reference: AEA 15925

To appear in: *Atmospheric Environment*

Received Date: 31 August 2017

Revised Date: 9 March 2018

Accepted Date: 27 March 2018

Please cite this article as: Beddows, D.C.S., Harrison, R.M., Identification of specific sources of airborne particles emitted from within a complex industrial (steelworks) site, *Atmospheric Environment* (2018), doi: 10.1016/j.atmosenv.2018.03.055.

This is a PDF file of an unedited manuscript that has been accepted for publication. As a service to our customers we are providing this early version of the manuscript. The manuscript will undergo copyediting, typesetting, and review of the resulting proof before it is published in its final form. Please note that during the production process errors may be discovered which could affect the content, and all legal disclaimers that apply to the journal pertain.

IDENTIFICATION OF SPECIFIC SOURCES OF AIRBORNE PARTICLES EMITTED FROM WITHIN A COMPLEX INDUSTRIAL (STEELWORKS) SITE

D.C.S. Beddows and Roy M. Harrison^{*†},

National Centre for Atmospheric Science
School of Geography, Earth and Environmental Sciences
University of Birmingham
Edgbaston, Birmingham B15 2TT
United Kingdom

^{*} To whom correspondence should be addressed.

Tele: +44 121 414 3494; Fax: +44 121 414 3708; Email: r.m.harrison@bham.ac.uk

[†] Also at: Department of Environmental Sciences / Center of Excellence in Environmental Studies, King Abdulaziz University, PO Box 80203, Jeddah, 21589, Saudi Arabia

ABSTRACT

A case study is provided of the development and application of methods to identify and quantify specific sources of emissions from within a large complex industrial site. Methods include directional analysis of concentrations, chemical source tracers and correlations with gaseous emissions. Extensive measurements of PM_{10} , $PM_{2.5}$, trace gases, particulate elements and single particle mass spectra were made at sites around the Port Talbot steelworks in 2012. By using wind direction data in conjunction with real-time or hourly-average pollutant concentration measurements, it has been possible to locate areas within the steelworks associated with enhanced pollutant emissions. Directional analysis highlights the Slag Handling area of the works as the most substantial source of elevated PM_{10} concentrations during the measurement period. Chemical analyses of air sampled from relevant wind directions is consistent with the anticipated composition of slags, as are single particle mass spectra. Elevated concentrations of PM_{10} are related to inverse distance from the Slag Handling area, and concentrations increase with increased wind speed, consistent with a wind-driven resuspension source. There also appears to be a lesser source associated with Sinter Plant emissions affecting PM_{10} concentrations at the Fire Station monitoring site. The results are compared with a ME2 study using some of the same data, and shown to give a clearer view of the location and characteristics of emission sources, including fugitive dusts.

Keywords: PM_{10} ; steelworks; Port Talbot; source identification; fugitive emissions

1. INTRODUCTION

The town of Port Talbot in South Wales has long been recognised as having some of the highest PM₁₀ concentrations in the United Kingdom (AQEG, 2011). Earlier source apportionment studies have shown the large integrated steelworks operating within the town to be an important contributor to elevated PM₁₀ levels (Taiwo et al., 2014a,b,c). Hayes and Chatterton (2009) analysed PM₁₀ data from Port Talbot and suggested that exceedences of the 24-hour PM₁₀ Limit Value (50 µg m⁻³) may be caused by a range of sources and conditions. It was concluded that the main sources contributing to elevated PM₁₀ were not from the blast furnaces and sinter plant stack, but rather due to wind-raised dust from the blending plant or from the most likely potential source 'activities' on the steelworks site listed as: Cambrian stone granulation; metal plating pits; furnace slag pits; multiserv briquetting; multiserv steel slag solidification/demetalling/cutting; multiserv scarfing activities; hot and cold mills; steel plant; demetalled BOS slag storage; furnace slag storage and crushing. This agrees also with the findings of Guinot et al (2016) who suggested - following their UV LIDAR study over a large integrated steel works in Spain - that air quality management of steelworks needs to focus on controlling large and coarse particle emissions, especially from open sources. Using positive matrix factorization, they identified mineral dust being predominant in all size fractions, with the steelworks being a clear source of carbonaceous species, and resulting in production of secondary inorganic aerosols. In particular, stack emissions were identified as a major contributor of fine particles, while open sources dominated the emissions of TSP, yielding up to 80% of particles larger than PM₁₀. UV lidar provided 2D maps of aerosols in real time, with an ability to detect PM emissions and to visualize complex plumes. For the Port Talbot Steelworks, Taiwo et al. (2014a) attributed 23% of PM₁₀ mass measured off-site to steelworks emissions from: blast furnaces (BF); basic oxygen furnace steelmaking plant

(BOS); and sinter unit, with the blast furnaces considered as the major contributor accounting for one-fifth of the PM_{10} mass. Coking and secondary aerosol accounted for 22% and traffic, marine and background aerosol accounted for 16%, 28% and 11% of the PM_{10} mass respectively. In addition, particle number concentration measurements by Taiwo et al. (2014c) showed that local emissions, probably from road traffic, dominated the smaller size bins (0.3–0.5 μm), while steelworks emissions dominated the range 0.5–15 μm , and for particles >15 μm marine aerosol appeared dominant.

75

Key trace elements attributed to the iron and steel industry include Cd, Cr, Cu, Hg, Ni, Se, V, and Zn, and analyses of airborne PM close to steel plants have shown that Fe, Mn, Zn, Pb, Cd and K are associated with emissions from the steel and iron plants (Kfoury et al., 2016; Gladtko et al, 2009). Kfoury et al. 2016 applied a constrained weighted-non-negative matrix factorisation model to $PM_{2.5}$ composition data collected in Dunkerque, Northern France in the vicinity of a steelworks. They identified 11 source profiles with various contributions; 8 were characteristics of coastal urban background site profiles and 3 were related to the steelmaking activities. Between them, secondary nitrates, secondary sulfates and combustion profiles give the highest contributions and account for 93% of the $PM_{2.5}$ concentration. The steelwork facilities contributed about 2% of the total $PM_{2.5}$ concentration and appeared to be the main source of Cr, Cu, Fe, Mn and Zn. Gladtko et al (2009) measured PM_{10} at four sampling sites in northern Duisburg; an area where iron and steel producing industry is concentrated. They showed calcium, iron and zinc measured at two sites close to the industrial area and information about the urban background aerosol was sufficient to calculate the PM_{10} contribution of the main single plants.

91

Focussing on specific sources, Hleis et al (2013) measured emissions directly from sources within a steelwork in Northern France using particle size distribution, chemical analysis, XRD, SEM-EDX and TGA/DTA. Samples collected from the sinter stack showed high levels of K and Cl^- , followed by Fe, NH_4^+ , Ca, Na and Pb. Conversely dust samples taken from the sinter cake discharge zone showed higher amounts of Fe, Ca and Al, and lower amounts of K, Cl^- , Na and Pb. Dust samples collected from the blast furnace (BF) and steelmaking cast house were distinguished from each other based on the higher levels of Fe (hematite and magnetite) and lower levels of Ca, Zn and C (graphite) found in BF dust. High levels of Ca and Fe were found in samples taken from the desulfurization slag processing area. Microscopic analysis of individual particles has also identified individual Fe-rich particles close to steel plants, e.g. Moreno et al. (2004) identified iron spherules in both fine and coarse PM fractions at the steelworks in Port Talbot, South Wales; Ebert et al. (2012) observed a significant fraction of individual iron oxides and iron mixtures in airborne PM near a steel industry in Duisburg, Rhine-Ruhr area, Germany.

Apart from the primary particulate pollutants discussed above, industries are also known for emission of gaseous pollutants such as carbon dioxide (CO_2), carbon monoxide (CO), sulphur dioxide (SO_2), nitrogen oxides (NO_x) and hydrogen gas (H_2), and volatile organic compounds (Tsai et al., 2008; Johansson and Soderstrom, 2011). Some of these gaseous pollutants can be transformed into secondary aerosols which are commonly detected in the atmosphere.

Although earlier studies have thrown useful light on the specific sources of particulate matter from within the South Wales steelworks site, this study was designed to provide more specific information on the emissions, which could inform mitigation strategies. It

provides a case study example of how a well-designed measurement programme can provide the data needed to develop cost-effective control options by identifying key sources of emission.

1.1 The Port Talbot Steelworks

The steelworks is sited on an area of $\sim 28\text{km}^2$ with a working area of $\sim 8\text{km}^2$. There are $\sim 50\text{km}$ of roads (many unsurfaced), $\sim 100\text{km}$ of railway and approximately 25,000 vehicle movements per day (Environment Agency Wales, 2009). Figure 1 presents a map of the Port Talbot steelworks and shows the locations of the different processes and the potential sources of particulate emissions which can be described as follows, according to Laxen et al. (2010):

- Stockyards (green and grey): Most of the raw materials of coal, coke and iron-bearing ores are imported through the deep water harbour and stored in one of the two main stockyards (ore to the north of the site and coal to the south). Raw materials including iron ores (FeO , Fe_2O_3 , Fe_3O_4), limestone (CaCO_3) and dolomite ($\text{CaMg}(\text{CO}_3)_2$) are used in a blast furnace (BF) once prepared within the sintering step, while lime (CaO) and fluorspar (CaF_2) are used in a BOS plant (Machemer, 2004). Fugitive dust from this area is expected to have components including Fe, Ca, Mg and Mn (Dall'Osto et al., 2012a).
- Coke Ovens (grey): Coal is carbonised to coke in a series of heated ovens with minimal air. Coals of differing properties are blended to form a coke with the required properties needed for the blast furnace. The heating process drives off volatiles and the coke is quenched and transferred by lorry (along Site Roads SR1-4 highlighted in the figure by red, amber and green) to the blast furnace. CO_2 , SO_2 , NO_x and soot

(particulate matter) are the main emission components. In the coke-making process, major elements observed by Tsai et al. (2007) in the emissions included S and Na.

- Sinter Plant (brown): Raw materials are blended in long beds and the sintering process produces a fused and partially reduced form of iron that can be used to make molten iron more efficiently. As a result, emission components of KCl, Fe, Pb, Zn and Mn are expected. KCl was also identified by Hleis et al., 2013 as a particulate dominating the emissions from the sintering process stack. Tsai et al. (2007) suggested that K and Pb which contribute a significant percentage (15 and 2%) to the total observed particle mass, are associated with the sintering process. Similarly, Oravisjarvi et al. (2003) found that the sinter plant contributed 96% and 95% of the total measured concentrations of Pb and Cd at Rahee, Finland.

- Blast Furnace (brown): Blast furnaces convert iron ores into molten iron using carbon, in the form of coal and coke. The molten iron is captured in 'torpedoes' (cylindrical rail cars) and the slag is either granulated (used in cement) or run into pits to cool, and subsequently crushed. Fe and Mn are components of the tapping process followed by Ca, Al, Si, S during the slag processing. Gaseous emissions of CO₂, SO₂, NO_x are also expected from the stove heating

- Basic Oxygen Steel-making (BOS) (pink): The 'torpedoes' transfer the molten iron to the BOS plant where it is converted to steel. This process produces desulph slag which is crushed. Fe, Zn, Pb and Mn are expected components. (Dall'Osto et al, 2008)

- Slag Handling Area SHA (yellow and blue): Slag from the BOS process is stored in pits and either reprocessed to extract residual metal and subsequently crushed (steel slag) or treated as waste. These areas are labelled SHA and encompass the following activities: furnace slag storage and crushing; Steel Slag Solidification, demetalling and cutting and demetalling BOS slag and storage.

- Hot and Cold Mills (pink): Steel slabs are heated and rolled into a long thin coil of metal. This is an energy intensive process. The hot forming process showed high abundance of S, Fe, Na and Ca (Tsai et al., 2007). The study of Machemer (2004) showed elevated concentration of Fe, Al, Si, S and Zn at sections in the vicinity of both BOS and BF.
- Power Plants (light blue): Producing steel is very energy intensive both in electricity and steam. Waste gases from the Coke Ovens and Blast Furnace are used as fuels.
- Site Roads SR1-6 (red,/amber/green). As to be expected, there is a network of roads on the site, some made and unmade, and despite mitigation strategies such as surface wetting and wheel washing, the regular usage of these roads by HGVs will lead to resuspension of dust. The roads with substantial traffic are coloured, green, orange and red in Figure 1.

2. METHOD

2.1 Measurement Sites

Port Talbot steelworks has eight council operated air quality monitoring sites positioned around the North and North East boundary of the Steelworks (see Table 1, www.welshairquality.co.uk). *Margam Fire Station* is the main monitoring site which is part of the DEFRA Automatic Urban and Rural Network (AURN) network. The monitoring station is within a self-contained, air-conditioned housing located within the grounds of a fire station and measures the main particulate and gaseous metrics. The nearest road is approximately 10 metres from the station and is an entrance to the steelworks. The nearest main road is the A48 or Commercial Road. It is a 30 mph road approximately 115 metres from the station with 10,000 vehicles per day (2012) comprising 82% cars; 11.5% Light Goods Vehicles LGVs; 3% Heavy Goods Vehicles HGV and 1.5% commercial

191 Passenger Carrying Vehicles PCVs. The M4 motorway is approximately 350 metres to the
192 NW with an annual average daily flow of 71,000 vehicles per day (averaged from 2014 to
193 2016 from Junction 39 to Junction 40 at Taibach). Of this 77.5 % are cars; 14.7 % LGV;
194 and 7.2 % HGV with the remaining 0.6 % made up of Two Wheeled Motor Vehicles
195 (TWMV) and PCV. The M4 is has 70 mph limit but as the road winds around Port Talbot a
196 50 mph speed limit is enforced by average speed cameras. The surrounding area is open
197 land associated with the steelworks and residential dwellings with a population of roughly
198 140,000 within the Neath-Port Talbot area. This equates to 317 people/km² compared to
199 632 and 2467 people/km² in Swansea and Cardiff respectively. Twll-yn-y-Wall, Talbot and
200 Theodore Road sites are roadside sites and only Twll-yn-y-Wall was included in this study
201 due to its closer proximity to the steelworks. Even though both the Talbot road and Twll-
202 yn-y-Wall sites are on the busy A48, Twll-yn-y-Wall Park is in a more open area compared
203 to the Talbot road site which could be considered a mini-street canyon. The Theodore
204 Road site is on a back street of Port Talbot and further away from the steelworks but much
205 closer to the M4. The other steel-work perimeter sites included the *Prince Street* site which
206 is within the open grounds of a quiet water pumping station. It is located next to the main
207 Swansea to London Paddington railway line on the side which is furthest from the
208 steelworks. This site is positioned the closest to the blast furnaces of the steelworks.
209 *Dyffryn School* (DS) is most Southerly site, exposed to emission from the mid section of
210 the steelworks with the closest source being the rolling mills. The site is next to the school
211 buildings but has a clear line of site - across playing fields and then over residential roof
212 tops - of the steelworks. Like Theodore Road, the DS site is close to the M4. Before the
213 opening (after this study) of the Port Talbot Distribution Road (PDR, designed to relieve
214 pressure on the M4 from local traffic) the *Docks* site was situated on a back road and was
215 described as an urban background site situated in an expanse. Although described as an

urban industrial site, the *Little Warren* site is situated on the the Southern tip of the residential areas of Sandfields and Aberafan and is alongside a footpath running along the mouth of the river Afan and Port Talbot Docks area. The closest source within the steelworks to the LW site is from the stock yards. Furthermore, on the South side of the estuary and on the coast is a break-water area where ships supplying the steelworks are unloaded. All meteorological data was collected from the Mumbles Head Observatory in Swansea (Met Office, 2012). It is positioned on a jut of land reaching out from the Southern coast of the Gower Peninsular into the Bristol Channel and Swansea Bay. It is roughly at a 10 km distance perpendicular to the coast running alongside Port Talbot steelworks.

2.2 Measurements

Each of the 8 sites (Table 1) collected measurements of PM_{10} around the site as part of the continuous monitoring programme carried out by Neath-Port Talbot Council. The monitoring site at Margam, FS is part of the national Automatic Urban and Rural Network (AURN) and in addition to PM_{10} , collected $PM_{2.5}$, O_3 , SO_2 , CO , NO_x , NO , NO_2 and meteorological (met) data. The met data comprised wind direction, wind speed, temperature, pressure, relative humidity and rainfall data. It was also at the FS that, our main lab was deployed to collect campaign data in April and May of 2012. The instruments deployed (Table 2) were used to collect chemical and physical data. Partisol-Plus dichotomous sequential samplers (Thermo Scientific, Model 2025)) and Digitel high-volume samplers (model DHA-80 Digitel Elektronik GA, Hagnau, Switzerland) were used to collect daily $PM_{2.5}$ and PM_{10} filters for laboratory measurement of cations/anions/EC/OC (Cl^- , NO_3^- , $nss-SO_4^{2-}$, Na^+ , NH_4^+ , K^+ , Mg^{2+} , Ca^{2+} , Al, V, Cr, Mn, Fe, Ni, Cu, Zn, Cd, Sb, Ba, Pb, EC and OC, see Taiwo et al 2014a for more details). The Partisol used 47 mm

diameter, PTFE filters whereas the Digitec was loaded with quartz filters. Partisols were also used to collect filters at the LW, PS and the LW sites. A Tecro Steaker sampler was used to collect hourly PM_{fine} and PM_{coarse} filter measurements, measured off line for elements (Na; Mg; Al; Si; S; Cl; K; Ca; Ti; Cr; Mn; Fe; Ni; Cu; Zn; Br; Sr; Pb) using PIXE analysis (Lucarelli et al., 2011). A second Streaker sampler was also operated concurrently at the LW site. We also collected BC data using a 7 wavelength Magee AE31 Aethalometer, single particle mass spectra using a TSI 3800 ATOFMS and particle number data using a Grimm 1.108 particle spectrometer (Taiwo et al., 2014c).

With regards to meteorological data, for the study period considered by our 2012 campaign, data was only available from the Mumbles Head Observatory (MU). Comparisons of this data set with the data measured at the Margam Fire Station (FS) site - for an augmented period with measurements at the FS - showed a close relationship between the wind directions with no offset. Modelled data was available at both the FS and Little Warren (LW) and this also gave a close relationship but with an offset of 15-20°. Similarly, there were linear correlations between the measured and modelled wind speeds measured at the three sites. Although, the wind speeds modelled at the LW and FS were 96% and 40% of the values measured at the MU. Hence data from MU was used throughout this analysis and was taken as representative of the conditions of the air moving over the steelworks. However, it was recognised that the topography of the land and buildings may affect the local movement of air around the site before arriving at the monitoring sites resulting in anomalies within the data.

2.3 Data Analysis

Bipolar plots of the metrics versus wind direction and wind speed provide the foundation of the first analysis carried out within this study. The bipolar plots were drawn using the Cran R package, Openair (Carslaw and Ropkins, 2012). Hotspots are often identified in the plots which show a range of wind directions and wind speeds where the measured metric is elevated, thus identifying a source. The code used to create these was further enhanced to add radial lines either sides of these hotspots. These marked a sector of wind directions across which the measurement metric rose above a statistic (eg 85th, 90th, 95th percentile). In addition to the bipolar plots being useful to identify sources which elevated the PM₁₀, bar plots were constructed from PM₁₀ measurements to show which chemical constituents or ME2 source factors (marine; secondary; traffic; steel1, steel2, steel3; sulphate, nitrate and background aerosol) derived from the constituents (Taiwo et al 2014a) contributed most to the elevation of PM₁₀. ME-2 is a least squares program for solving multi-linear problems. Specifically, it solves bilinear problems taking the form $X = G \cdot F + E$. X is a matrix whose rows contain the hourly/daily measured chemical species which is factorised into a combination of source factors F and their corresponding time series G; matrix E is a remainder term. We were also able to provide supporting data from ART2a cluster analysis of ATOFMS data and k-Means analysis of Grimm particle size data.

283

3. RESULTS

The results presented are structured to further our understanding of the measurements of common air pollutants made by the national monitoring (AURN) network around the steelworks. The gas and PM measurements are considered and used to identify the most likely source areas giving rise to the elevated concentrations of PM. This is then extended using campaign data collected in 2012 at the Little Warren and Fire Station sites. In this,

two stories unfold, one which points to the Slag Handling area of the site, and another which points towards the steel making processes.

3.1 Gases

At the Margam Fire Station AURN site, gaseous and particulate metrics are measured continuously and include: NO; NO₂; NO_x; O₃; SO₂; CO; PM_{2.5} and PM₁₀. When the average mass concentrations of the AURN gases are banded according to four ranges of PM₁₀ (3-19; 19-35; 35-56; and 56-141 µg/m³) and then plotted, NO, NO₂ and NO_x are observed to rise with PM₁₀ up to a PM₁₀ concentration of 50 µg/m³ (Table S1). O₃ shows no trend with PM₁₀ but SO₂ and CO continue to rise with PM₁₀ above 50 µg/m³ suggesting that the sources associated with the higher PM₁₀ concentrations are also linked to SO₂ and CO emissions. Similarly for the meteorological data (Table S2), higher PM₁₀ values are more likely for higher wind speeds and for wind directions between 186 and 227°, which are directions in line with the northern and southern boundary of the Slag Handling area (labelled as SHA in Figure 1). Although a general increase in PM₁₀ with wind speed suggests a windblown dust source, 'hot-spots' within the wind roses have been observed within this sector which suggests an influence of process sources (e.g. Steel and Slab, Ironmaking).

Road activity and fugitive dusts from material handling and storage are expected to make a significant contribution to PM alongside Stack and Diffuse emissions from plant processes, e.g. Sinter and BOS plant (Tata Steel, personal communication). When viewed from the AURN site at Margam Fire Station, any PM contribution due to the road activity through the Slag Handling Area is in the shadow of the region of the Blast Furnaces which will also

314 make a contribution in this wind sector. The Slag Handling Area represents the combined
315 area used to process the slag generated from iron and steel making.

316

317 The pollution roses (for NO, NO_x and CO) in Figure S1 all show a hot spot for wind
318 directions (209-232°) from the south west of the monitoring station and for elevated wind
319 speeds between 7 and 18 m/s. NO_x and CO appear most probably to be a combination of
320 the emissions from the Sinter Plant and Blast Furnaces. However, this angle of wind
321 direction encompasses not only the Sinter Plant and Blast Furnaces, it also encompasses
322 the road emission sources passing along the coastal roads (orange SR1 and red SR2) and
323 through the Slag Handling Area. It is referred to as Meteorology Case 1. Likewise, PM_{2.5},
324 PM₁₀ and SO₂, (Figure S2) are elevated in concentration for wind speeds between 7 and
325 18 m/s, albeit for a similar range of wind directions rotated slightly clockwise to include
326 more of the emissions from the Sinter Stock source and their roads (green SR4)– referred
327 to as Meteorology Case 2. Also, within this sector area around the blast furnace are three
328 areas marked in yellow. These, from West to East include: the Coal Injection Plant;
329 Granulation Activities and the Furnace Slag Pits. SO₂ is more likely to be an emission
330 from the Sinter Plant accompanied by fugitive dusts from within the vicinity, e.g. from the
331 conveying of raw materials. It might also be expected that PM arises from raw materials
332 containing heavy metals associated with the sintering process,(e.g. Zn, Pb and Cd),
333 where some may be volatilised directly or converted into volatile compounds, e.g.
334 chlorides, seen in the ATOFMS cluster 13 K-Cl, with possible Cd and Pb peaks (at m/z
335 110-114 and 208 respectively; Figure S3), and occurs in the flue gas. Non-volatile and
336 volatile PM_{2.5} are measured using the TEOM FDMS and the non-volatile fraction makes up
337 most of the PM_{2.5} and has a similar windrose. The volatile fraction is different, in that

points towards the SSE, possibly influenced by regional transport of semi-volatile ammonium nitrate.

3.2 Particulate matter (PM) mass

Figure 2 shows concurrent PM_{10} measurements at the LW and the FS sites constraining the emission to high speed winds (10-15 m/s) passing over the Blast Furnaces, Sinter Plant, Slag Handling area and Ore Stock Yard. Comparing the two PM_{10} wind roses for the Little Warren and Margam Fire Station sites, the maximum hourly PM_{10} value measured was 35 and 210 $\mu g/m^3$ respectively. The larger spread of wind directions associated with high concentrations at the LW compared to the FS site is best explained by a line source which is perpendicular to the line of sight to LW and in line with the FS site. When the wind blows across the line source towards LW, the PM_{10} rises to a maximum of 35 $\mu g/m^3$ at any one point along the line source and arriving at the LW site within the acceptance angle α . However, when the wind blows along the line source, there is approximately a six-fold increase in concentration of PM_{10} to in excess of 210 $\mu g/m^3$ over smaller acceptance angle β . The two PM_{10} wind roses constrain the emission area to the upper part of the Slag Handling area, the Sinter Plant and the more northerly Blast Furnace. The non-volatile PM_{10} shows a similar directional association to the PM_{10} wind rose but the volatile PM_{10} emissions are in the direction of the mill and off-site sources and like volatile $PM_{2.5}$ make a small contribution to the PM_{10} of 5 $\mu g/m^3$.

The source area is constrained further to just the Slag Handling area when considering PM_{10} measurements from the Docks and Dyffryn School (Figure 3) and if a line source is suspected as being responsible for the elevated emission then one of the roads passing through the Slag Handling Area is a good candidate. Figure 3 superimposes onto the map

the PM₁₀ wind roses calculated for the six sites considered and for each wind rose two radial lines are marked where the PM₁₀ concentration is at the 90 percentile (PM₁₀ = 38 µg/m³ at FS). Bipolar plots for Talbot Road and Theodore Road are given in Figure S4. These were omitted from the analysis due to their locations, i.e. being within a mini canyon and close proximity to the M4 motorway respectively. However, in spite of this, a retrospective view of the data collected at these two sites supports the conclusions derived from the other Port Talbot sites. Using the pairs of radial lines for each site, two extreme areas can be marked out shown by the black and grey boundaries. The grey and black boundaries represent the minimum and maximum source area, respectively, for which the PM₁₀ concentration is over the 90 percentile. Addition of the PM₁₀ wind roses collected at Prince Street and Twll-yn-y-Wal Park to this plot complements this observation and the aerial view (<https://www.google.co.uk/maps/@51.571154,-3.78268,16z>) underneath the black boundary clearly shows a grey dusty handling area which is in sharp contrast to the black and brown rust dust areas around other operations on site. This is a different result to that presented in the AQEG (2011) report "Understanding PM₁₀ in Port Talbot", which circles the area east of the Slag Handling area which includes: Blast Furnaces and Slab Yards.

To visualise the magnitude of the PM₁₀ values in these pollution roses, Figure 4 shows the values of the maximum PM₁₀ values for these sites. For all of the sites, over half of the time, the PM₁₀ is below 20 µg/m³ (cf 2012 annual mean of 18 µg/m³ at both Swansea Road in Swansea (*lat* = 51°37'57.706"N, *long* = 3°56'50.546"W) and Cardiff Central (*lat* = 51°28'54.408", *long* = 3°10'34.500"W)). But at the FS and PS sites, there is a notable high percentage of occurrence of PM₁₀ values above 20 µg/m³. The PS site records the highest PM₁₀ values and the Docks the lowest. The magnitudes measured at the different

sites can be understood by considering the distance between these sites and the various sources. In particular, there is a distinct PM_{10} -distance relationship when considering the area in and around the Slag Handling Area (see Figure 5a). The mean PM_{10} value correlates with the inverse distance to the receptor sites from the centre of the Slag Handling Area. This relationship remains when considering the maximum PM_{10} values as a function of inverse distance from the Slag Handling area. The maximum values measured at Dyffryn School (DS) and Twll-yn-y-Wal (Twll) do not fit this linear trend but the measurements are brought into line when considering the 90th percentile (Figure 5b,c).

When considering the wind roses at the LW and FS expressed as Conditional Probability Functions (Uria-Tellaetxe and Carslaw, 2014), the contribution of the steelworks source become significant for the 75-100th percentile of data (Figure 6a). This corresponds to PM_{10} values between 23-99 and 27-210 $\mu g/m^3$ for the LW and FS sites respectively. For percentile ranges below 75% the CPF wind roses point away from the steelworks (Figure 6b). This gives a clear indication that for the campaign period, a source within the area bounded by the bold line in Figure 6a was responsible for the high PM_{10} values. It is also worth mentioning that at the LW site, the main source detected is from the West (from sea spray) due to its close proximity to the coast, and in comparison, there is less than 60 % conditional probability that the elevated PM_{10} at the LW is from the direction of the steelworks. A comparable strong Westerly source from the sea is not observed at the FS.

3.2.1 AURN data (PM_{10}) corrected for upwind background

Further results are obtained by estimating the increment due to the steelworks which can be considered by measuring the difference between the foreground (Downwind) and background (Upwind) sites (Figure S5 and S6). Two cases are presented. In Cases 1

and 2, the PM_{10} measurements from the LW and FS sites are selected by wind direction 162-270° and 100-152° respectively and each set is averaged. In Case 1, the wind direction is from the sea passing over the steelworks. For this, the LW is the Upwind and the FS is the Downwind site. For Case 2, the wind direction is along the coast and wind directions are chosen such that the LW measures the increment above the FS which pertains to the steelworks. A clear increase in PM_{10} (11 $\mu\text{g}/\text{m}^3$) and Non-Volatile PM_{10} can be seen for case 1 (Figure S5, where only PM_{10} was measured at LW). There is no change in Volatile PM_{10} suggesting that the rise in PM_{10} is more likely from wind-blown dust. This same increment is observed for Case 2 where LW is downwind of the FS site (see Figure S7) together with an effect due to the traffic along the M4 motorway raising NO_x and $PM_{2.5}$ to higher values than those seen in Case 1.

3.3 Chemical Measurements

3.3.1 Streaker/PIXE Data

The increment in PM can be further examined using the chemical composition measured using hourly Streaker/PIXE measurements (Figure S7, S8, S9 and S10). For Case 1, the wind blows from the sea, across the Slag Handling area, Sinter Plant and Blast Furnaces to the Fire Station site. Comparing the Streaker/PIXE data measured at the Fire Station with the Streaker/PIXE data measured at Little Warren, an increase in all fine and coarse elements is seen (except for fine Na and Cl). There is a notable increase in S, Ca and Fe in both size fractions and Na, Cl, Mg, Al and Si in just the coarse fraction. For Case 2, the same comparison between downwind and upwind Streaker/PIXE data, is not as clear-cut. An elevation in fine Na, Ca, K, S and Fe and only coarse Ca and Fe is seen with a marginal increase in Si. When this analysis is repeated for wind directions passing over the Slag Handling area (Figure S10), an enhancement is seen in fine Ca, Fe, K, Mn and

Zn and coarse Al, S, Ca, Fe and Si for Case 1 (when the wind blows along the length of the source) and in fine Na, Mg, Al, S, Cl, K, Ca, Fe and Sn and coarse Na, Mg, Al, S, Cl, Ca, Fe and Si in Case 2 (when the wind blows across the source). For the purpose of this comparison, the LW data have been scaled by a factor of 2.1 to allow for enhanced dilution (compared to FS) during transport from the Slag Handling Area (based on findings illustrated in Figure 5). Fine K, Ca, Fe and Zn are all enhanced for both Case 1 and 2. However, Ca and in particular Fe, are considerably enhanced for Case 1. In comparison with the work of Taiwo et al. (2014b) this is characteristic of the Blast Furnace Factor (see below, ME2 section). For the coarse measurements, the main components that are enhanced are S (in Case 1), Ca, Si and Fe. This is consistent with emissions from a line source passing through the Slag Handling area whose main components are enhanced Fe, Ca and Si.

The contribution of each of these elements for various PM_{10} concentration ranges is shown in Figure 7a. Fe is clearly a key constituent elevating the PM_{10} followed by Ca and S. The contribution of these elements to the PM_{10} rises from less than 10% to 50% for the 56-141 $\mu\text{g}/\text{m}^3$ range. There are also significant contributions from Na, Mg and Cl. Figure 7b shows the same result but for wind speed suggesting that during the campaign the source is not from a process source but from a wind driven source, e.g. surface dust on a road. The contribution of Fe and Ca only increases for wind speeds above 6 m/s.

3.3.2 ME2 Results

Considering the ME2 source apportionment results derived from the Streaker/PIXE data by Taiwo et al. (2014a) (Figure 8), all factors contribute to the elevation of PM_{10} , namely, Steel 1 and Steel 3, followed by Sintering, Steel 2, Marine and Background Aerosol.

Again, all wind-driven sources are shown in Figure 8b Steel 1, 2 and 3 are associated with Blast Furnace, Coking Process and BOS plant respectively. The Steel 1 source is characterised by high concentrations of both Ca and Fe; Steel 2 is characterised by high levels of Fe, Ca, Na and Zn; Steel 3 is high in sulphur; and Steel 4 has high concentrations of Ca, Si and Al. Steel 1 and Steel 3 make the highest contribution to the elevation of PM_{10} and have time series with a high correlation to PM_{10} mass (0.7 compared to less than 0.13 for the other factors) indicating that they are possibly from the same source or area of wind blow dust, comprised largely of Fe, Ca and S.

3.3.3 Effect of Rainfall

If windblown dust is suspected as being responsible for the elevation of PM_{10} , then changes in the PM according to rainfall might be expected. Figures S11a and S11b show how the PM_{10} values varied for all 8 Port Talbot sites. Average values fall with increased rainfall as a general trend. The difference in the Streaker/PIXE data measured on a dry day compared to a wet day again consistently shows an elevation of Ca and Fe in the fine and coarse modes on dry days. Coarse sea salt elements (Na, Mg and Cl) are all enhanced on a dry day together with Al, Ca, K and Fe (Figure S11d). Fine Ca and Fe are also enhanced on a dry day together with elements Mg, Al, S, Cl, K, Ti, Mn, Zn and Pb (Figure S11c).

3.3.4 Correlation with AURN Trace Gases

The correlation of these Streaker/PIXE measurements with the gaseous pollutants measured at FS site has also been considered. Table S3 shows the correlation coefficient calculated between the Streaker/PIXE increments and the gas measurements collected at the Fire Station site. There is no significant correlation for meteorology Case 2, but for

488 Case 1 we see strong correlations between: SO₂ and fine K, Al, Fe, Pb, Mn, Se and S;
489 SO₂ and coarse K, Ca, Al, Fe, Cr, Pb, Ti, Mn and S. Likewise, there are strong
490 correlations between CO and fine Mg, K, Ca, Al, Fe, Zn, Pb, Mn, Se and S; and CO and
491 coarse K; Ca; Al; Fe, Zn, Cr, Ti, Mn and S. Figure S12 plots these relationships, showing
492 the strongest relationships between fine and coarse Fe, Ca and S with SO₂ and CO.
493 These results are presented graphically for SO₂ and CO in the columns of the correlation
494 plots in Figure S13. In these plots, high correlation between SO₂ and fine K, Pb, S and
495 Se; CO and fine Al, Ca, Cl, Fe, Mn, Pb, S, Se, Ti and Zn; SO₂ and coarse Al, Cl, Fe, K,
496 Mg, Mn, Na, Pb, S and Ti; and CO and coarse Ca, Cr, K, Mg, Mn, Na, Ti and Zn are
497 observed. Also, natural groupings amongst the fine and coarse Streaker/PIXE elements
498 are seen. For example, in the fine fraction, a grouping of fine Fe, Al, Ca, Mn, S, Se and Ti
499 and coarse Fe, Ca, Cl, Cr, K, Mg, Mn, Pb, S and Ti are seen. Interestingly, Ni and Cr have
500 the lowest or negative correlations. It seems likely that the elements associated with fine
501 particles may arise from the same source of process emissions as the SO₂ and CO
502 (presumably the sinter plant and blast furnaces) while the coarse fraction metals more
503 probably arise from the area in and around the Slag Handling area, which is on the same
504 wind sector from the sampler.

505

506 3.5 ATOFMS

507 There have been a number of earlier deployments of the Aerosol Time-of-Flight Mass
508 Spectrometer (ATOFMS) at Port Talbot, reporting measurements of metallic (Dall'Osto et
509 al., 2008a) and non-metallic (Dall'Osto et al., 2012b) species, and the full range of
510 particles (Taiwo et al., 2014b).

511

Table 3 presents a summary of the results of the ART2a analysis of the ATOFMS mass spectra collected during the four week campaign (details are in Taiwo et al., 2014b) at the FS site. From this, a general background made up of the first main clusters 1-5 consisting of regional nitrate, sulphate, sea salt and EC is seen. Not reflecting the mass detected, these ATOFMS clusters account for ~80% of the number of detected particles. The remaining 20% can be attributed to sources within and around Port Talbot and are associated by polar plots with high counts for winds from the SW with high speed, i.e. wind-blown sources, namely clusters 6, 7, 9, 13, 14 and 16 (Figures S3a and S3b). The polar plots of clusters 6 and 7 point to several sources in the south of the site (similar to Met. Case 2) and include the: Blast Furnaces; Slag Handling Areas (SHA 3-4); Metal Plating pit; BOS plant; Coke Ovens and Site Roads (SR 1-4). The polar plots for clusters 9, 13 and 16 (Met. Case 1) include the: Power Plants; Blast Furnaces; Sinter Plant; Slag Handling Areas (SHA 1-3); Metal Plating pit; Coke Ovens and Site Roads (SR 2-4 and 6). Cluster 14 is peculiar in that it has a very narrow angle of occurrence and neatly encompasses the Furnace Slag Pits. It had the chemical signature of Amines as a single 24 hour episode of particles with a 2.0 μm mode. Clusters 9, 13 and 14 have wind roses which point towards the Blast Furnaces and Slag Handling area whereas clusters 6 and 7 have wind roses which are more associated with winds passing over the southern part of the steelworks (including Slab Yards 1 and 2 and the Coal Stock Yard). The behaviour of these clusters suggests wind-blown dust but their composition suggests a steel-making process. The wind roses of each of these clusters point towards the same region of the Slag Handling areas marked in Figure 3. Cluster 9 is interesting in that it has a road traffic signature and the wind rose points to an area covering all of the Slag Handling region and Ore Stock Yard. In combination, clusters 13, 14 and 16 suggest a source with contributions from the following constituents: Na, K, Fe,

Cd, Pb, S, CN, Cl, NO₃, SO₄ and PO₃ all of which can be associated with Blast Furnace and/or Sinter Plant emissions. Without a second ATOFMS operating at a second site (such as the LW), or a library of ATOFMS data collected from each of the sources on site to carry out a Discriminant Analysis, it is difficult to isolate sources. Hence, with ATOFMS data, we can conclude the influence of two types of dust areas (to the SW and SSW of the FS) and vehicle emissions encompassing the main site roads (SR 1-4).

3.6 Physical Measurements

3.6.1 Overview of the Data

Particle size distributions were measured during the campaign using a Grimm Dust Monitor v1.108. This was operated at the Fire Station site and the average results are presented in Figure 9. To differentiate between the steelworks (wind sector 270° through 0° to 140°) and background (wind sector 270° through 180° to 140°), two wind sectors were considered (figure 9a). The number distribution (Figure 9b) was converted to volume ($dV/d\log(D_p)$) and revealed four modes with modal diameters $D_p = 0.3, 0.9, 2.0$ and $5.0 \mu\text{m}$. Furthermore, the modes centred at $2.0 \mu\text{m}$ and $5.0 \mu\text{m}$ can be seen to be elevated when the wind sector includes the steelworks. Hence it can be concluded that this may be the mode which is contributing to the elevation of PM_{10} at the FS site. Figure 10a considers the volume distributions for various PM_{10} ranges from 0 to $61 \mu\text{g}/\text{m}^3$ and shows that as PM_{10} increases, the modes fitted at 2.2 and $4.5 \mu\text{m}$ both increase, the latter with a slightly higher gradient. Figure 10b confirms that both the 2.2 and $4.5 \mu\text{m}$ modes contribute to the elevation of PM_{10} whereas the smaller modes in the distribution do not.

3.6.2 K-Means Cluster Analysis

561 A general overall picture of the particle volume size distribution spectra can be obtained by
562 analysing the hourly spectra using *k*-Means cluster analysis (see Beddows et al. (2009) for
563 methodology). This resulted in six clusters whose frequency is shown in Figure S14a.
564 The Cluster Proximity Diagram (Figure S14b) shows how the clusters are arranged
565 according to their similarity to each other; similar clusters are placed close to one another
566 whereas dissimilar clusters are placed far apart. Figure S15 shows the average particle
567 volume spectrum of each cluster together with the diurnal cycle of the cluster and the wind
568 rose associated with that cluster. The most frequent clusters are distinguished from each
569 other as being steelworks and background spectra. Cluster 1 and 2 have strong peaks at
570 2.5 μm compared to the 5.5 μm peak. Cluster 1 occurs during the day and for wind
571 directions passing over the Ore Yard, Slag Handling Plant, Sinter Plant and Blast
572 Furnaces. Cluster 2 is strongest for wind directions blown from inland and occurs mainly at
573 night. Clusters 5 and 6 do not have a clear diurnal pattern but are strongest for inland
574 winds passing over the M4 motorway which is probably reflected in the high mode below
575 0.5 μm . Clusters 3 and 4 are more interesting because they are both daytime clusters and
576 occur for wind directions passing over the Slag Handling area and Ore Yard respectively.
577 Both clusters have elevated modes at both 2.5 and 5.5 μm suggesting a characteristic of
578 the line source elevating PM_{10} .
579 The composition of these clusters can be derived using the Streaker data collected at the
580 LW and FS sites. Cluster 1 is associated with elevated Sea Salt (coarse Na, K, Mg and
581 Cl) but is also accompanied by a significant increment from dust (coarse Al and Ca) and
582 Fe and S in the fine and coarse mode (Figure S16). These same increments are not as
583 pronounced for the background cluster, cluster 2 and considering the different wind
584 directions, it is clear that S, Ca and Fe are higher when the wind blows across the site.
585 Small increments in Fe and Ca are observed for cluster 3 with significant increases in S

and BC but for a narrow wind sector passing over the Slag Handling area. There is also an unexpectedly high measurement of Zn at LW, possibly from a wind direction blowing across a source at the South of the site. Considering the wind rose, with its high speed westerly winds, cluster 4 is a strong steelworks cluster and this is supported by the strong enhancement of fine S, Ca, Fe and BC and coarse Mg, Al, S, K, Ca and Fe. Clusters 5 and 6 are interesting in that they show a very strong increment of sulphur in both the fine and coarse ranges although considered to be a background cluster. This is probably regional sulphate pollution due to long-range transport.

3.6.3 Contributions to PM₁₀

From the findings of this work, it can be seen that both process emissions and wind-blown dusts are responsible for the elevation of PM₁₀. Using SO₂ as a marker of process emissions and the sum of the Grimm size bins from 3 to 20 µm as a metric for resuspended dust an estimation of the contribution of each to PM₁₀ can be assessed by regressing PM₁₀ upon SO₂ and Dust all normalised to their maximum value. Equation 1 shows the result of this regression.

$$\frac{PM_{10}}{\max(PM_{10})} = 0.53 \times \frac{SO_2}{\max(SO_2)} + 0.41 \times \frac{\text{Dust}}{\max(\text{Dust})} + 0.043$$

This suggests that both process emissions and wind-blown dusts make a similar contribution to the elevation of PM₁₀. In fact when regressing PM₁₀ against SO₂, NO_x, CO and Dust, the regression factors are 0.44, 0.03, 0.1 and 0.40 confirming the major contributors to PM₁₀ as a process or processes also emitting SO₂ and wind-blown dust. The former probably include the blast furnaces and sinter plant.

4. CONCLUSIONS

610 Campaign data sets collected in April and May of 2012 around the Port Talbot steelworks
611 have been further analysed. Hayes and Chatterton (2009).concluded that the PM_{10}
612 exceedences within the Port Talbot conurbation were most likely to be from fugitive dusts
613 arising from within the steelworks. In particular, emissions from vehicular movement on
614 the roads on the site and emissions from the material storage and handling appeared to be
615 likely candidate sources. Our campaign data provide quantitative evidence in relation to
616 those sources

617

618 Considering the AURN gas data measured at the sites in Port Talbot, wind roses of the
619 trace gases measured at the FS site identify two source directions covering either the
620 Blast Furnaces and the whole of the Slag Handling area (NO , NO_x , O_3 and CO) or the
621 Sinter Plant and the more Northern parts of the Slag Handling area (SO_2 , $PM_{2.5}$, and
622 PM_{10}). It is the second case which includes wind directions yielding the higher PM
623 concentrations which are of interest in this work to understand the elevation of PM_{10} . Plots
624 showing the Streaker/PIXE data vs these trace gases show that Fe and Ca have a positive
625 dependence although not a significant correlation compared to other metrics.

626

627 When including receptor sites additional to the main AURN site at the FS, characteristics
628 of the source(s) of PM are observed. The maximum PM_{10} concentration measured at the
629 FS is six times higher than the maximum PM_{10} measured at Little Warren and this
630 difference can be accounted for by an inverse relationship between the PM_{10} value and the
631 distance between the centre of the Slag Handling area and receptor sites. Also there is a
632 large difference in the spread of wind directions for each site when PM_{10} concentrations
633 are highest (LW and FS) which can be explained by a line source passing perpendicular to
634 the LW site and toward the FS site. Inclusion of PM_{10} wind rose data collected at the Port

635 Talbot Docks, Prince Street, Twll-yn-Wall and Dyffryn School sites supports the conclusion
636 that a line source through the Slag Handling area is largely responsible for the elevation of
637 PM_{10} . Furthermore, when considering the PM_{10} wind rose in terms of conditional
638 probability at the LW and FS, it is clearly seen that elevations of PM_{10} above the upper
639 quartile of data (19 and 24 $\mu g/m^3$ for LW and FS respectively) are most likely to occur
640 when the wind blows from the coast and over the steelworks. If the PM_{10} is less than the
641 upper quartile of PM_{10} then is most likely that the wind is blowing from the sampling sites
642 towards the steelworks. This is also consistent with a source on the steelworks site - most
643 likely a line source within the Slag Handling area – being largely responsible for the
644 elevation of PM_{10} in Port Talbot.

645

646 When dividing the data according to wind speed and PM_{10} concentration, an elevation of
647 PM_{10} for wind speeds above 6 m/s is observed. Considered as a moderate breeze, a wind
648 of 6 m/s will cause dust and loose paper to be raised off the ground and into the air. At
649 this wind speed, small waves on the sea will become larger and fairly frequently ‘white
650 horses’ giving rise to sea salt spray are observed. Using the Streaker/PIXE data, the
651 elevation of PM_{10} can be attributed in part to sea salt but is mainly associated with Fe and
652 Ca. We also see an increase in sulphur although it does not make a significant
653 contribution to the PM_{10} mass. The ME2 sources identified by Taiwo et al. (2014a), by
654 receptor modelling of the same data, point the responsibility for elevated PM_{10} towards
655 their Steel 1 and Steel 3 factors which were attributed to the Blast Furnaces and Coking
656 processes. These factors have a large association with Fe, Ca and S but are also linked
657 to Mg, Al, Si, Ti and Mn for the case of Steel 1 and Cu and Pb for Factor 4 implying that
658 they are more likely from a wind-blown dust arising within the area in and around the Slag
659 Handling area rather than a direct process emission. Again, the increase of PM_{10} with wind

660 speed is consistent with a resuspension source compared to a constant process source
661 which is more likely to decrease in concentration with increasing wind speed.
662 Furthermore, the PM_{10} data measured at the receptor site closest to the Slag Handling
663 area, and in line with a potential line source (i.e. at the FS), show a decrease in
664 concentration with increased rainfall. This provides further support for a resuspension
665 source because the same observation is not made at receptor sites furthest away from the
666 Slag Handling area and perpendicular to a potential line source. Differences between 'wet'
667 and 'dry' days at the FS site show an increase in coarse Na, Cl, Ca and Fe on the 'dry'
668 days. Similarly, fine Ca, Mg, Al, S, Cl and notably Fe increase on 'dry' days. Further
669 support for a wind-blown dust source can be derived from the particle size-volume spectra
670 measured at the FS where four modes are identified in the data, centred at 0.35, 0.89, 2.2
671 and 4.5 μm , and it is the latter two coarse modes which are correlated to PM_{10} mass.

672

673 Considering the coarse particle Streaker/PIXE data, Fe and Ca are highly correlated to Mg
674 and Mn which are characteristic of a stockyard fugitive dust but they are not as strongly
675 correlated to CO and SO₂ giving further confidence that the source is associated with
676 wind-blown dust rather than a process emission such as coking or power generation.
677 There are further strong correlations of Fe and Ca to Al and S which indicate a source
678 consistent with a wind-blown dust from the Slag Handling Area. There are also strong
679 correlations to Cr, Mg, Mn, and Ti. Fe also has its own additional strong correlation to Pb,
680 K and Cl which is characteristic of a Sinter Plant dust which may also be contributing to a
681 smaller extent to the elevation of PM_{10} . The absence of silicon within the PIXE analysis of
682 the Streaker data makes it difficult to explicitly link the chemical profile to a Slag Handling
683 process.

684

685 Analysis of the qualitative ATOFMS data (particles aerodynamic diameter < 3.5 μm)
686 collected at the Fire Station showed that the most frequently detected particles (by
687 number) were from background sources such as sea salt, regional sulphate, regional
688 nitrate and elemental carbon. Following these in magnitude were clusters of particles with
689 signals from PAHs, metals, phosphate, copper, chloride and sulphur which were all
690 attributable to the steelworks. Out of these clusters, those whose wind rose pointed
691 towards the Slag Handling area contained coarse Fe, Ca, Si, K, Cl, CN, phosphate and S,
692 elements expected to be characteristic of slag handling. There was also a 24 hour
693 episode from this wind direction which contained a 2.0 μm mode of amines. Also worth
694 noting was that PAH and Fe-PO₃ clusters were most associated with southerly wind
695 directions. As a postscript to the ATOFMS reanalysis, although ART2a cluster analysis
696 was used to find the most natural groups within the data, the full potential of this high
697 resolution data may not have been realised. The use of Discriminant Analysis to assign
698 the data collected during the campaign to source specific profiles derived by at-source
699 measurements, e.g. the Slag Handling area, Blast Furnaces, Sinter Plant, etc. may be
700 more fruitful using a nozzle inlet with a much higher upper size range.

701

702 A number of other studies have reported measurements of particulate pollution in the
703 vicinity of steelworks, located in northern France (Hleis et al, 2013) Kfoury et al, 2016),
704 southern France (Sylvestre et al, 2017), northern Spain (Ameida et al, 2015; Guinot et al,
705 2016) and northern Germany (Gladtkke et al, 2009). Both Sylvestre et al (2017) and
706 Kfoury et al (2016) focus upon the PM_{2.5} size fraction. As in our study, the steelworks
707 does not make a major contribution to this size fraction (about 2% in the case of Kfoury et
708 al, 2016), with metals being significant contributors to the emissions. Hleis et al (2013)
709 characterise the chemical profiles from different sources, and as noted above, these are

consistent with our own findings and assisted in identifying source areas. Both Almeida et al (2015) and Gladtko et al (2009) found major contributions to PM_{10} from the blast furnaces and sinter plant. In the former case, chemical profiles broadly similar to our own were reported (Almeida et al, 2015), while in the latter, Ca, Fe and Zn were considered sufficient to estimate PM_{10} contributions from the main plants. Our analysis provides a more detailed characterisation, hence allowing differentiation between the sources, Guinot et al (2016), differentiated between process (stack), fugitive and open sources emissions by use of lidar and a PMF study based upon measurements of chemical composition. In terms of contributions to TSP, open sources (40%) were the largest contributor, followed by stack (18%) and fugitive (10%), on top of the regional pollution (32%). Open sources described wind blown dusts, and the blast furnace slagging process was noted as a particular source, consistent with our own observations.

In conclusion, the analysis presented shows that the steelworks is responsible for the upper quartile of measured PM_{10} at the FS AURN site. PM_{10} wind roses locate the source within the Slag Handling area and the varied range of wind directions over which PM_{10} is high at the FS and LW sites suggest a line source. Furthermore, there is a strong correlation between the upper 90 percentile of PM_{10} concentrations and the inverse distance between all of the receptor sites around the steelworks and the centre of the Slag Handling area. The particles are within the coarse mode of the volume distribution and their elevation with increased wind speed and decrease with rainfall suggest that a wind-blown dust rather than a process emission is responsible. The chemical composition associated with the source has strong contributions from Fe and Ca which are characteristic of a dust from the steelworks, and most likely the Slag Handling process.

734 There is also a contribution from particulate matter from a process also emitting sulphur
735 dioxide, probably the blast furnaces and/or sinter plant.

736

737 Prior to this study, the specific sources of particles within the steelworks had long been
738 unclear (AQEG, 2011), hence delaying fully effective control measures. The study shows
739 how it is necessary to apply a range of complementary methods to give a clear picture of
740 the emission sources, and that this complements and extends the insights gained from
741 application of the ME2 model.

742

743 **ACKNOWLEDGEMENTS**

744 The authors are grateful to the Welsh Government for funding the additional data analyses
745 reported in this paper.

REFERENCES

- Almeida, S.M., Lage, J., Fernandez, B., Garcia, S., Reis, M.A., Chaves, P.C., 2015. Chemical Characterisation of atmospheric particles, and source apportionment in the vicinity of a steel making industry. *Sci. Tot. Environ.*, 511-512, 411-420.
- AQEG, 2011. Air Quality Expert Group. Understanding PM₁₀ in Port Talbot. Advice note prepared for Department of Environment, Food and Rural Affairs: Scottish, Welsh Assembly Government, and Department of the Environment, Northern Ireland.
- Beddows, D.C.S., Dall'Osto, M., Harrison, R.M., 2009. Cluster analysis of rural, urban and curbside atmospheric particle size data. *Environ. Sci. Technol.*, 43, 4694-4700.
- Carslaw, D.C. and Ropkins, K., 2012. *Openair* - an R package for air quality data analysis. *Environ. Modell. Softw.*, 27-28, 52-61.
- Dall'Osto, M., Booth, M.J., Smith, W., Fisher, R., R.M. Harrison, 2008a. A study of the size distributions and the chemical characterisation of airborne particles in the vicinity of a large integrated steelworks. *Aerosol Sci. Technol.*, 42, 981-991.
- Dall'Osto, M., Booth, M.J., Smith, W., Fisher, R. and Harrison, R.M., 2008b. A study of the size distributions and the chemical characterisation of airborne particles in the vicinity of a large integrated steelworks. *Aerosol Sci. Technol.*, 42, 981-991.
- Dall'Osto, D., Drewnick, F., Fisher, R., Harrison, R.M., 2012a. Real-time measurements of nonmetallic fine particulate matter adjacent to a major integrated steelworks. *Aerosol Sci. Technol.*, 46, 6, 639-653.
- Dall'Osto, M., Drewnick, F., Fisher, R., Harrison R.M., 2012b. Real-time measurements of non-metallic fine particulate matter adjacent to a major integrated steelworks. *Aerosol Sci. Technol.*, 46, 639-653.
- Ebert, M., Müller-Ebert, D., Benker, N., Weinbruch, S., 2012. Source apportionment of aerosol near a steel plant by electron microscopy. *J. Environ. Monit.*, 14, 3257-3266.
- Environment Agency Wales, 2009. Port Talbot Steelworks PM Permit Review.
- Gladtko, D., Volkhausen, W., Bastian, B., Estimating the contribution of industrial facilities to annual PM₁₀ concentrations at industrially influenced sites. *Atmos. Environ.* 43 (2009) 4655-4665.
- Guinot, B., Gonzalez, B., Perim De Faria, J., and Kedia, S., Particulate matter characterization in a steelworks using conventional sampling and innovative lidar observations. *Particuology* 28 (2016) 43-51.
- Hayes, E. and Chatterton, T., 2009. An independent review of monitoring measures undertaken in Neath Port Talbot in respect of particulate matter (PM₁₀), Report prepared for the Welsh Assembly Government by the University of the West of England, Bristol.

- Hleis, D., Fernández-Olmo, I., Ledoux, F., Kfoury, A., Courcot, L., Desmonts, T., and Courcot, D., Chemical profile identification of fugitive and confined particle emissions from an integrated iron and steelmaking plant. *Journal of Hazardous Materials* 250– 251 (2013) 246–255.
- Johansson, M.T., Söderström, M., 2011. Options for the Swedish steel industry - Energy efficiency measures and fuel conversion. *Energy*, 36, 191-198.
- Kfoury, A., Ledoux, F., Roche, C., Delmaire, G., Roussel, G. and Courcot, D. PM 2.5 source apportionment in a French urban coastal site under steelworks emission influences using constrained non-negative matrix factorization receptor model, *J. Environ. Sci.*, 40 (2016) 114–128.
- Laxen, D., Moorcroft, S., Marner, B., Laxen, K., Boulter, P., Barlow, T., Harrison, R.M., Heal, M., 2010. PM_{2.5} in the UK. Project ER12 Final Report. www.aqconsultants.co.uk/AQC/.../Reports/SNIFFER-PM25-Rept-Final-201210.pdf [Last accessed 18 Aug 2017].
- Lucarelli, F., Nava, S., Calzolari, G., Chiari, M., Udisti, R., Marino, F., 2011. Is PIXE still a useful technique for the analysis of atmospheric aerosols? The LAB Experience. *X-Ray Spectrom.*, 40, 162-167.
- Machemer, S., D., 2004. Characterization of airborne and bulk particulate from iron and steel manufacturing facilities. *Environ. Sci. Technol.*, 38, 381-389.
- Met Office, 2012. Met Office Integrated Data Archive System (MIDAS) Land and Marine Surface Stations Data (1853-current). NCAS British Atmospheric Data Centre, date of citation, 2012. <http://catalogue.ceda.ac.uk/uuid/220a65615218d5c9cc9e4785a3234bd0> [Last accessed 18 Aug 2017].
- Moreno, T., Jones, T.P. and Richards, R.J., 2004. Characterisation of aerosol particulate matter from urban and industrial environments: examples from Cardiff and Port Talbot, South Wales, UK. *Sci. Total Environ.*, 334-335, 337-346.
- Oravisaarvi, K., Timonen, K.L., Wiikinkoski, T., Ruuskanen, A.R., Heinanen, K., Ruuskanen, J., 2003. Source contributions to PM_{2.5} particles in the urban air of a town situated close to a steel work. *Atmos. Environ.*, 37, 1013-1022.
- Sylvestre, A., Mizzi, A., Mathiot, S., Masson, F., Jeffrezo, J.L., Dron, J., Mesbah, B., Wortham, H., Marchand, N., 2017. Comprehensive chemical characterization of industrial PM_{2.5} from steel industry activities, *Atmos. Environ.*, 152, 180-190.
- Taiwo, A., Beddows, D., Calzolari, G., Harrison, R.M., Lucarelli, F., Nava, S., Shi, Z., Valli, G. and Vecchi, R., 2014a. Receptor modelling of airborne particulate matter in the vicinity of a major steelworks site. *Sci. Tot. Environ.*, 490, 488-500.
- Taiwo, A.M., Harrison, R.M., Beddows, D.C., Shi, Z., 2014b. Source apportionment of single particles sampled at the industrially polluted town of Port Talbot, United Kingdom by ATOFMS. *Atmos. Environ.*, 97, 155-165.

- 845 Taiwo, A.M., Beddows, D.C.S., Shi, Z., Harrison, R.M., 2014c. Mass and number size
846 distributions of particulate matter components: Comparison of an industrial site and an
847 urban background site. *Sci. Tot. Environ.*, 475, 29-38.
- 848
- 849 Tsai, J.-H., Lin, K.-H., Chen, C.-Y., Ding, J.-Y., Choa, C.-G. and Chiang, H.-L., 2007.
850 Chemical constituents in particulate emissions from integrated iron and steel facility. *J.*
851 *Hazard Mater.*, 147, 111-119.
- 852
- 853 Tsai, J.-H., Lin, K.H., Chen, C.-Y., Lai, N., Ma, S.Y. and Chiang, H.-L., 2008. Volatile
854 organic compound constituents from an integrated iron and steel facility. *J. Hazard.*
855 *Mater.*, 157, 569-578.
- 856
- 857 Uria-Tellaetxe, I., Carslaw, C.D., 2014. Conditional bivariate probability function for source
858 identification. *Environ. Modell. Softw.* 59, 1-9.
- 859
- 860

TABLE LEGENDS

Table 1 Monitoring sites placed around the perimeter of Port Talbot steelworks (2012).

Table 2 Instrument Augmentation by Birmingham University (May 2012).

FIGURE LEGENDS

Figure 1 Map of Port Talbot showing the sources areas. The black targets indicate the positions of the monitoring site listed in Table 1. Modified from Laxen et al., 2010.

Figure 2 Maps showing the areas of potential sources creating high concentrations of PM_{10} measured at the Little Warren (LW) and Port Talbot Margam AURN (FS) sites. The schematic shows the possible position of a line source relative to the LW and FS and the angles of high PM from this with $\alpha > \beta$. [Plotted using data measured during campaign 18 April-16 May 2012. Red and blue lines mark the 95 and 90 percentile directions respectively, PM_{10} units: $\mu g/m^3$].

Figure 3 Wind roses identifying the cross sectioned area on the map as an area of most likely sources of PM_{10} that contribute to high concentrations. [Plotted using data measured during campaign 18 April-16 May 2012, PM_{10} units: $\mu g/m^3$]. Upper diagram shows the triangulation (using wind directions with PM_{10} greater than the 90th percentile) used to prescribe the source area and the lower diagram shows the aerial photograph of the area. [Little Warren (LW), Port Talbot Margam AURN (FS), Port Talbot Docks (DOCKS), Prince Street (PS), Twll-yn-y-Wall (Twll) and Dyffryn School (DS) sites].

Figure 4 Comparison of maximum PM_{10} measured at the six sites (FS-Fire Station; LW-Little Warren; DS – Dyffryn School; DOCK –Port Talbot Docks; PS – Prince Street; Twll – Twll-yn-y-Wal). The colours show what the fraction of the height of the bar represents the frequency of occurrence of the PM_{10} range of values. [Plotted using data measured during campaign 18 April-16 May 2012].

Figure 5 Comparison of PM_{10} measured at the six sites (FS-Fire Station; LW-Little Warren; DS – Dyffryn School; DOCK –Port Talbot Docks; PS – Prince Street; Twll – Twll-yn-y-Wal] around Port Talbot. Mean and maximum values plotted against distance from the centre of the Slag Handling area ($lat = 51^{\circ}, 34', 16.154''N$, $long = 3^{\circ}, 46', 57.648''W$, -). [Plotted using data measured during campaign 18 April-16 May 2012.16 May 2012]. (a) mean PM_{10} ; (b) maximum PM_{10} ; (c) 90%th percentile PM_{10}].

Figure 6 Conditional probability wind roses showing (a) the 75-100 percentile range of PM_{10} values (LW = 23-99 and FS = 27-210 $\mu g/m^3$) (b) the 0-75 percentile range of PM_{10} values (LW = 0-23 and FS = 0-27 $\mu g/m^3$). [Colour scale

represents the conditional probability from 0 to 1 as colours from blue through to red].

Figure 7 Bar chart showing the elemental composition of the average PM_{10} value for four ranges spanning the full range of (a) PM_{10} concentrations and (b) Wind speed measured at the Fire Station AURN site. [Grey hatched area indicates the fraction of the PM_{10} not accounted for by the Streaker measurements]. [Units: $\mu g/m^3$] [Quartile range of wind speeds used, m/s].

Figure 8 Bar charts showing the composition as described by ME2 factors by Taiwo et al. (2014a) of the average PM_{10} concentrations for four ranges spanning (a) the full range of PM_{10} concentrations and (b) wind speed measured at the Fire Station AURN site. [Grey hatched area indicates the fraction of the PM_{10} not accounted for by the Streaker measurements]. [Quartile PM_{10} and speed ranges used, $\mu g/m^3$, m/s].

Figure 9 Analysis of Grimm data: (a) map showing sectors representing the steelworks and background; (b) number size distribution [units: $1/cm^3$]; (c) volume size distribution [units: $\mu m^3/cm^3$].

Figure 10 (a) Relationship between area under the curves to measured mean PM_{10} ; (b) same data plotted for individual modes within the Grimm size distribution data. Two largest modes with modal diameters at 2.2 and 4.5 μm have the highest correlation with PM_{10} and have been associated with an FeP particle type from Hot and Cold Mills by Dall'Osto et al. (2008b). [units: $dV/dLogDp - \mu m^3/cm^3$].

938 **Table 1.** Monitoring sites placed around the perimeter of Port Talbot steelworks (2012).

Site	Lat	Long	*PM ₁₀	*PM _{2.5}	O ₃	SO ₂	CO	NO _x	NO ₂	NO	Met
Little Warren (LW)	51 : 35' : 5.748" N	3 : 48' : 3.848" W	✓19 µg m ⁻³								✓**
Port Talbot Docks (DOCKS)	51 : 35' : 24.839" N	3 : 47' : 9.776" W	✓18 µg m ⁻³								
Talbot Road	51 : 35' : 29.324" N	3 : 46' : 45.109" W	✓22 µg m ⁻³								
Theodore Road	51 : 35' : 23.791" N	3 : 46' : 19.218" W	✓19 µg m ⁻³								
Margam Fire Station (FS)	51 : 35' : 2.220" N	3 : 46' : 14.959" W	✓23 µg m ⁻³	✓	✓	✓	✓	✓	✓	✓	✓
Prince Street (PS)	51 : 34' : 46.762" N	3 : 45' : 59.274" W	✓23 µg m ⁻³	✓							
Twl-yn-y-Wal Park (TWLL)	51 : 34' : 36.034" N	3 : 45' : 32.418" W	✓23 µg m ⁻³								
Dyffryn School (DS)	51 : 34' : 20.759" N	3 : 45' : 3.931" W	✓16 µg m ⁻³								
Mumbles Head (MU)	51 : 33' : 54.000" N	3 : 58' : 51.600" W									✓

*PM10 measured with TEOM FDMS and hence split into non-volatile and volatile fraction. Figure next to tick mark is the Annual Mean for 2012.

Annual mean for 2016 given for PS.

** Modelled data.

939

940 **Table 2.** Instrument Augmentation by Birmingham University (May 2012).

Site	Partisol 2025	PCR TECTORA Streaker	Digitel DHA-80	ATOFMS TSI 3800	Aethalometer AE31	GRIMM Dust Monitor v1.108
Little Warren (LW)	✓	✓				
Margam Fire Station (FS)	✓	✓	✓	✓	✓	✓
Prince Street (PS)	✓					
Dyffryn School (DS)	✓					

941

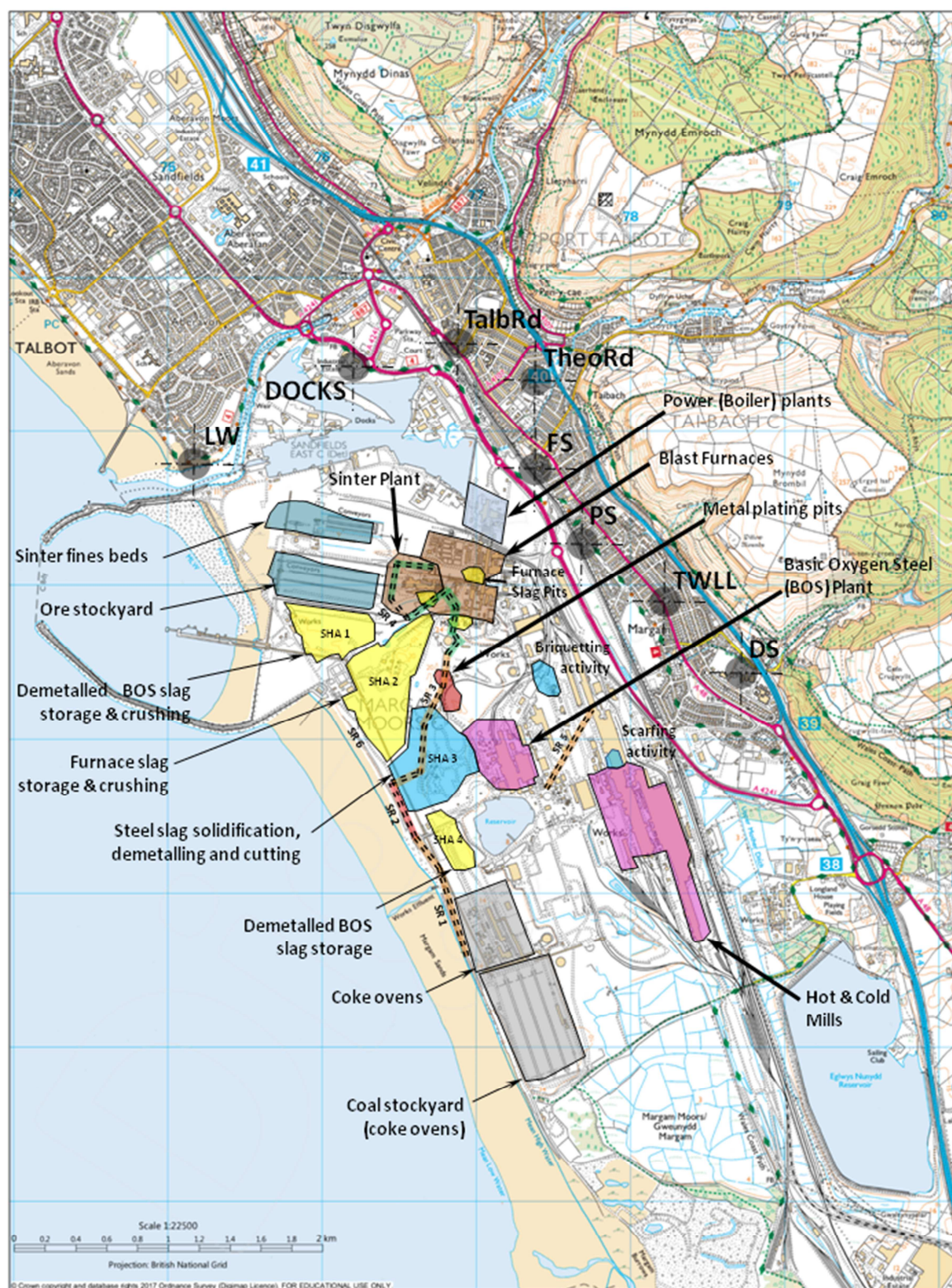
942

943 **Table 3.** Summary of ATOFMS clusters derived using ART2a analysis.

944

Cluster Number	Type	Characteristic	% Counts	Comments
1	K-NO ₃	Regional Nitrate	25.1	Local and NE winds
2	EC	Regional EC	31.5	Local
3	NaCl	Sea Salt	9	Local
4	NaK-CN	Dust?	8.5	Local and W Winds
5	KSO ₄	Regional Sulphate	5	Local and W Winds
6	PAH	PT	7.5	S winds, no clear diurnal trend
7	FePO ₃	PT Phosphate	7.5	S winds, peaks at 6am and 1pm
8	SOA	Traffic	2	NE Winds, strong at night.
9	Ca-EC	Lub oil from roads	1	SW winds, high during 6:00-21:00.
10	FeNO _x	FeNit	0.6	Local, strong at 5am.
11	K-EC	Traffic	0.6	NE winds, strong in afternoon and evening
12	K-SO ₄	Traffic	0.6	NE winds, strong in afternoon and evening
13	KCl – Unique	PT Chloride	0.5	SW winds, no clear diurnal trend
14	Amines	Amines 24hr episode	0.4	SW winds, no clear diurnal trend
15	Copper	PT – Copper	0.1	SW winds, Strong at 4-5am.
16	Sulphur	PT – Sulphur	0.1	Local and SW winds, strong at midday.

945



© Crown Copyright/database right 2011. An Ordnance Survey EDINA supplied service.

Figure 1. Map of Port Talbot showing the sources areas. The black targets indicate the positions of the monitoring site listed in Table 1. Modified from Laxen et al., 2010.

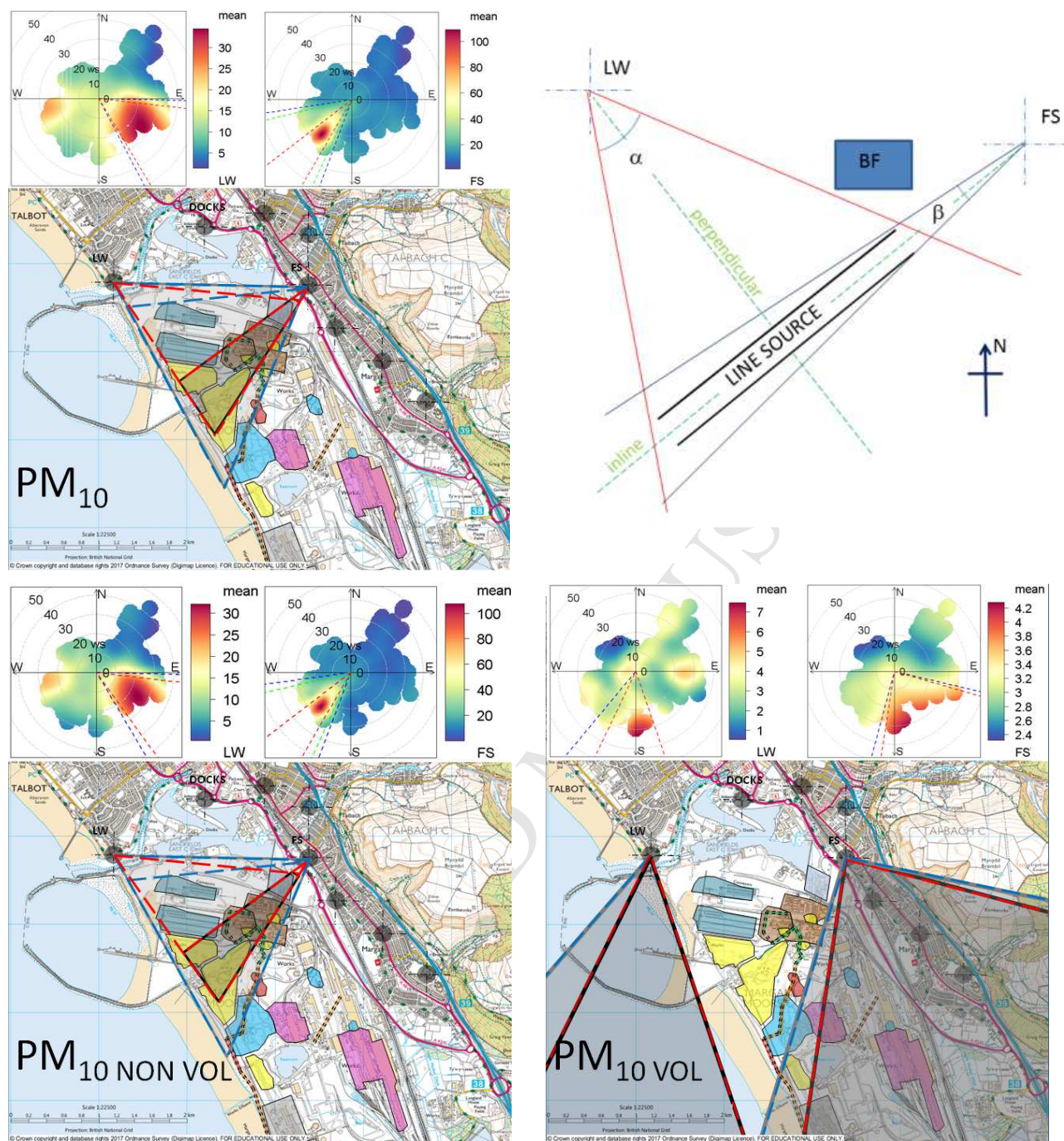
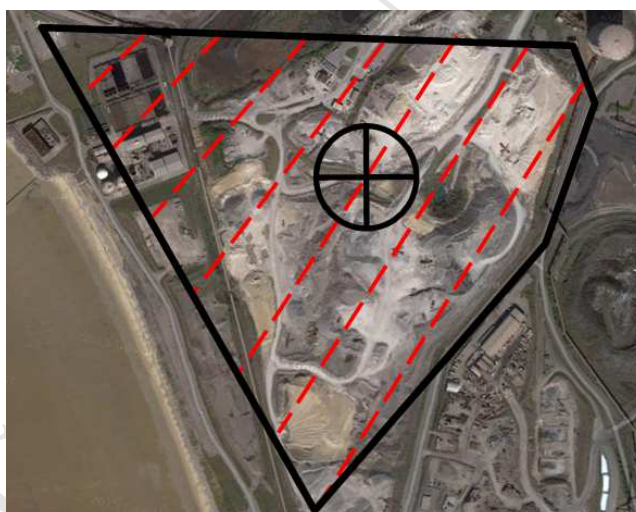
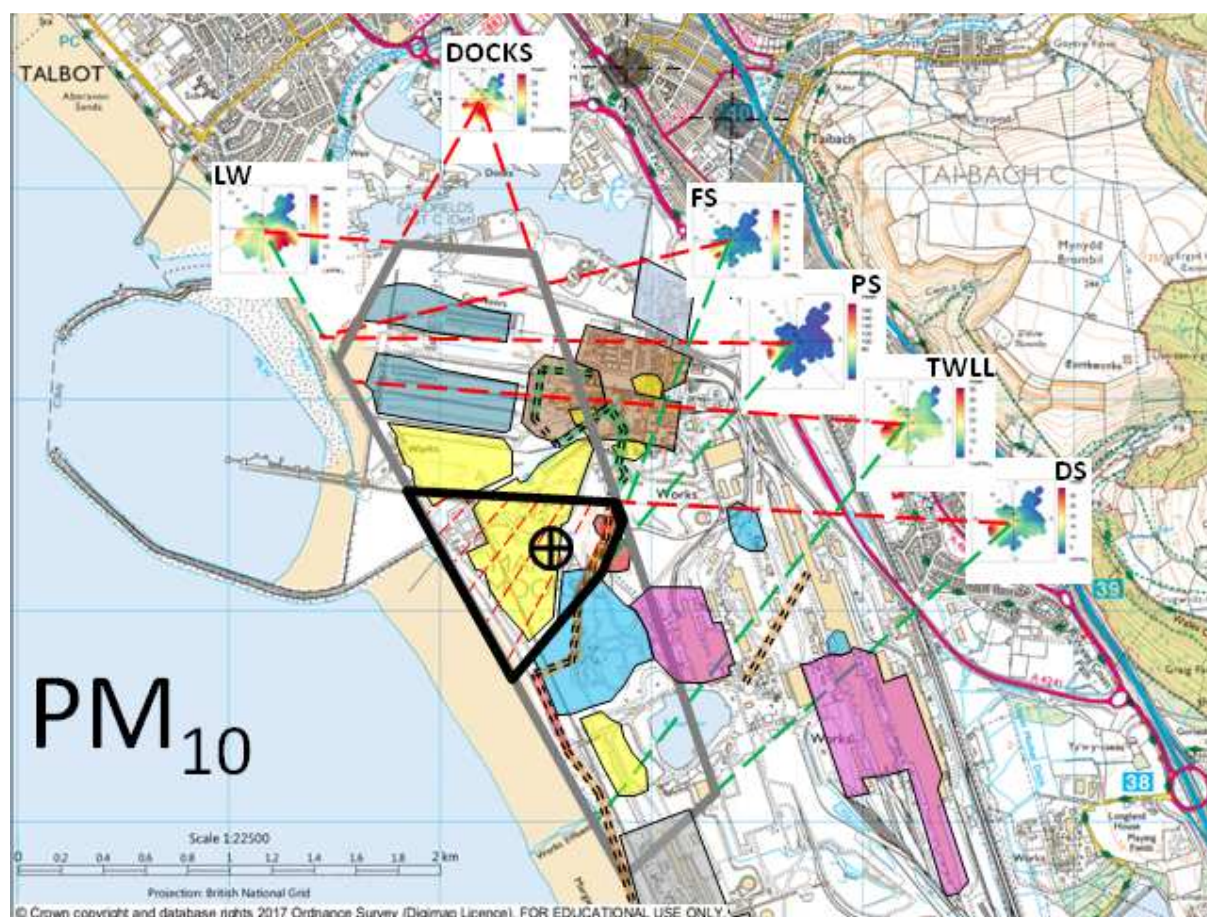


Figure 2. Maps showing the areas of potential sources creating high concentrations of PM₁₀ measured at the Little Warren (LW) and Port Talbot Margam AURN (FS) sites. The schematic shows the possible position of a line source relative to the LW and FS and the angles of high PM from this with $\alpha > \beta$. [Plotted using data measured during campaign 18 April-16 May 2012. Red and blue lines mark the 95 and 90 percentile directions respectively. PM₁₀ units: $\mu\text{g}/\text{m}^3$].

946
947



<https://www.google.co.uk/maps/@51.571154,-3.78268,16z>

Figure 3. Wind roses identifying the cross sectioned area on the map as an area of most likely sources of PM_{10} that contribute to high concentrations. [Plotted using data measured during campaign 18 April-16 May 2012, PM_{10} units: $\mu g/m^3$]. Upper diagram shows the triangulation (using wind directions with PM_{10} greater than the 90th percentile) used to prescribe the source area and the lower diagram shows the aerial photograph of the area. [Little Warren (LW), Port Talbot Margam AURN (FS), Port Talbot Docks (DOCKS), Prince Street (PS), Twll-yn-y-Wall (Twll) and Dyffryn School (DS) sites].

948

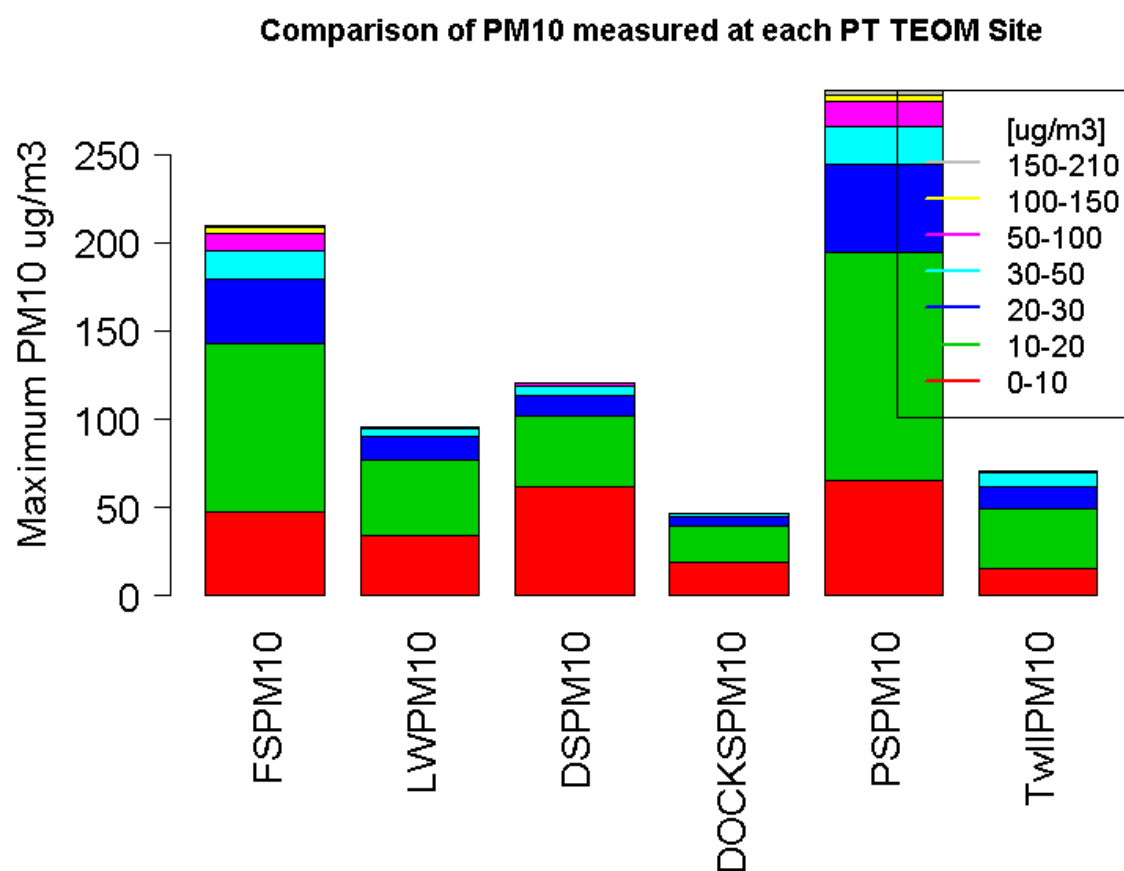


Figure 4. Comparison of maximum PM₁₀ measured at the six sites (FS-Fire Station; LW-Little Warren; DS – Dyffryn School; DOCK –Port Talbot Docks; PS – Prince Street; Twll – Twll-yn-y-Wal). The colours show what the fraction of the height of the bar represents the frequency of occurrence of the PM₁₀ range of values. [Plotted using data measured during campaign 18 April-16 May 2012].

949
950
951
952
953
954
955
956
957
958
959

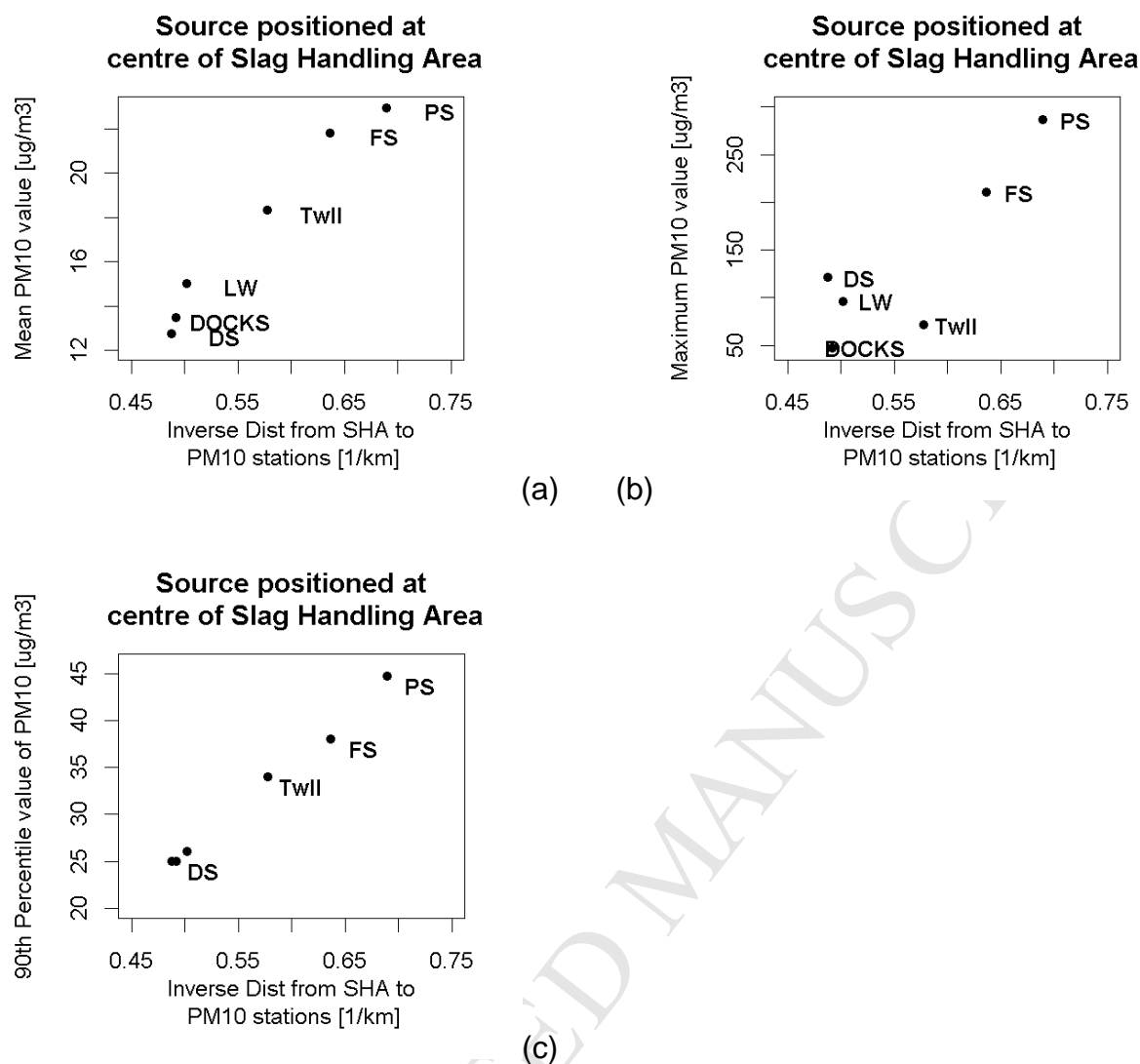


Figure 5. Comparison of PM₁₀ measured at the six sites (FS-Fire Station; LW-Little Warren; DS – Dyffryn School; DOCK –Port Talbot Docks; PS – Prince Street; Twll – Twll-yn-y-Wal] around Port Talbot. Mean and maximum values plotted against inverse distance (1/km) from the centre of the Slag Handling area (*lat* = 51°34'16.154"N, *long* = 3°46' 57.648"W). [Plotted using data measured during campaign 18 April-16 May 2012.16 May 2012]. (a) mean PM10; (b) maximum PM10; (c) 90%th percentile PM₁₀.]

960
961
962
963
964

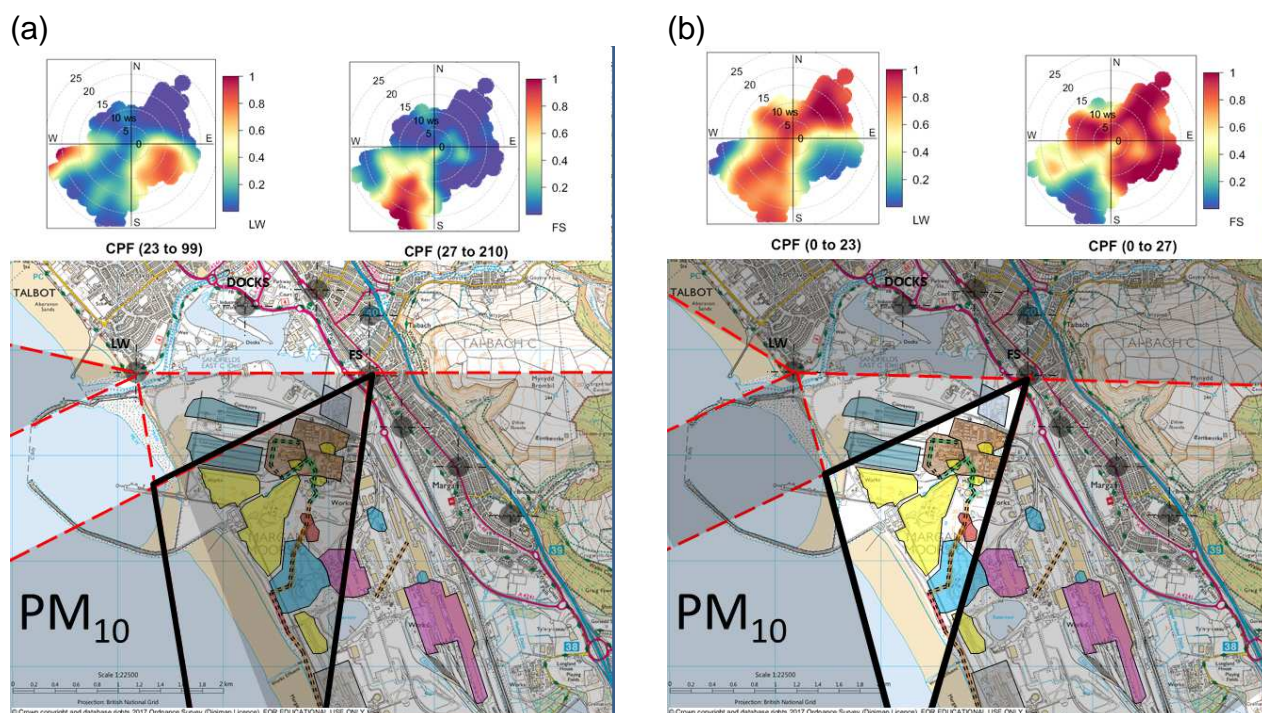


Figure 6. Conditional probability wind roses showing (a) the 75-100 percentile range of PM_{10} values (LW = 23-99 and FS = 27-210 $\mu g/m^3$) (b) the 0-75 percentile range of PM_{10} values (LW = 0-23 and FS = 0-27 $\mu g/m^3$). [Colour scale represents the conditional probability from 0 to 1 as colours from blue through to red].

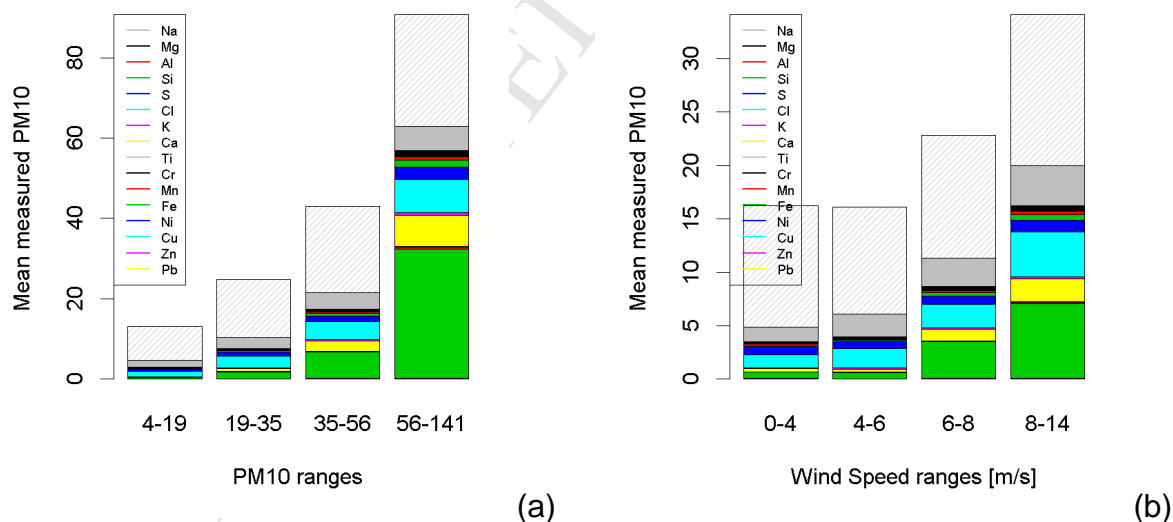


Figure 7. Bar chart showing the elemental composition of the average PM_{10} value for four ranges spanning the full range of (a) PM_{10} concentrations and (b) Wind speed measured at the Fire Station AURN site. [Grey hatched area indicates the fraction of the PM_{10} not accounted for by the Streaker measurements]. [PM_{10} units: $\mu g/m^3$] [Quartile range of wind speeds used, m/s].

970

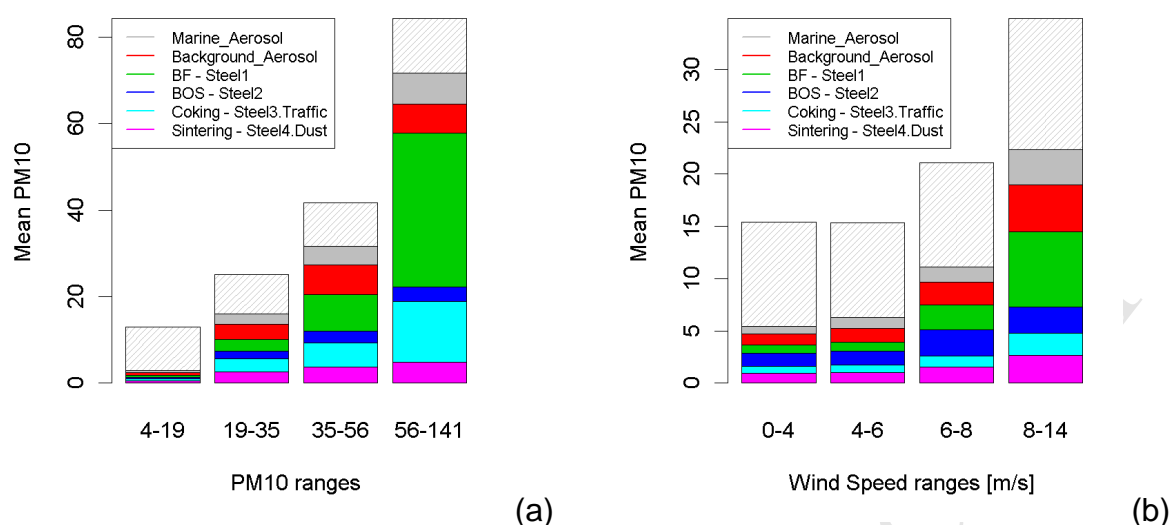


Figure 8. Bar charts showing the composition as described by ME2 factors by Taiwo et al. (2014a) of the average PM₁₀ concentrations for four ranges spanning (a) the full range of PM₁₀ concentrations and (b) wind speed measured at the Fire Station AURN site. [Grey hatched area indicates the fraction of the PM₁₀ not accounted for by the Streaker measurements]. [Quartile PM₁₀ and speed ranges used, $\mu\text{g}/\text{m}^3$, m/s].

971
972
973
974
975
976
977
978
979
980
981
982
983
984

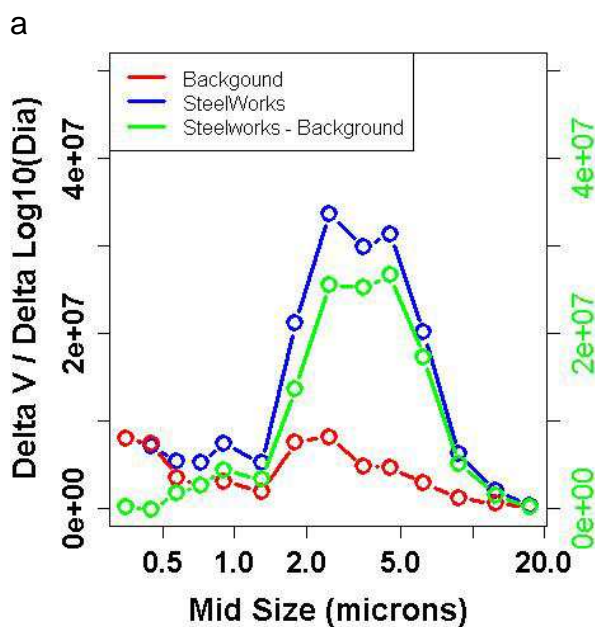
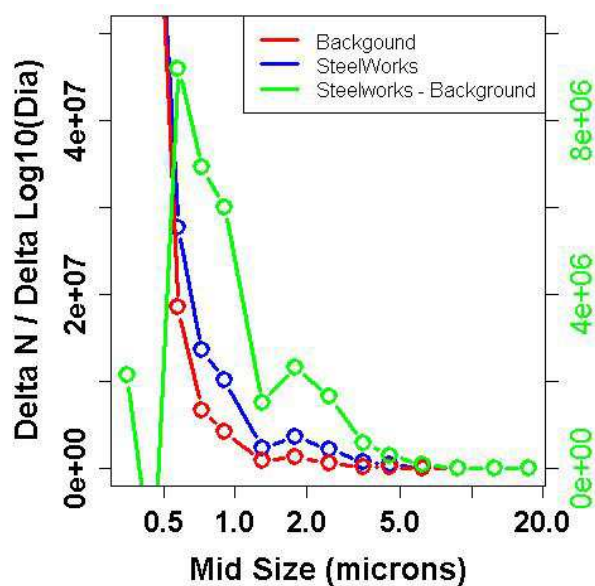
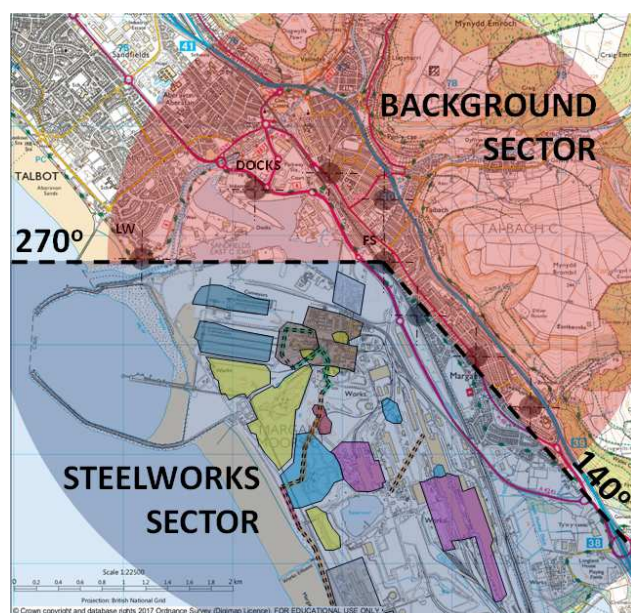


Figure 9. Analysis of Grimm data: (a) map showing sectors representing the steelworks and background; (b) number size distribution [units: $1/\text{cm}^3$]; (c) volume size distribution [units: $\mu\text{m}^3/\text{cm}^3$].

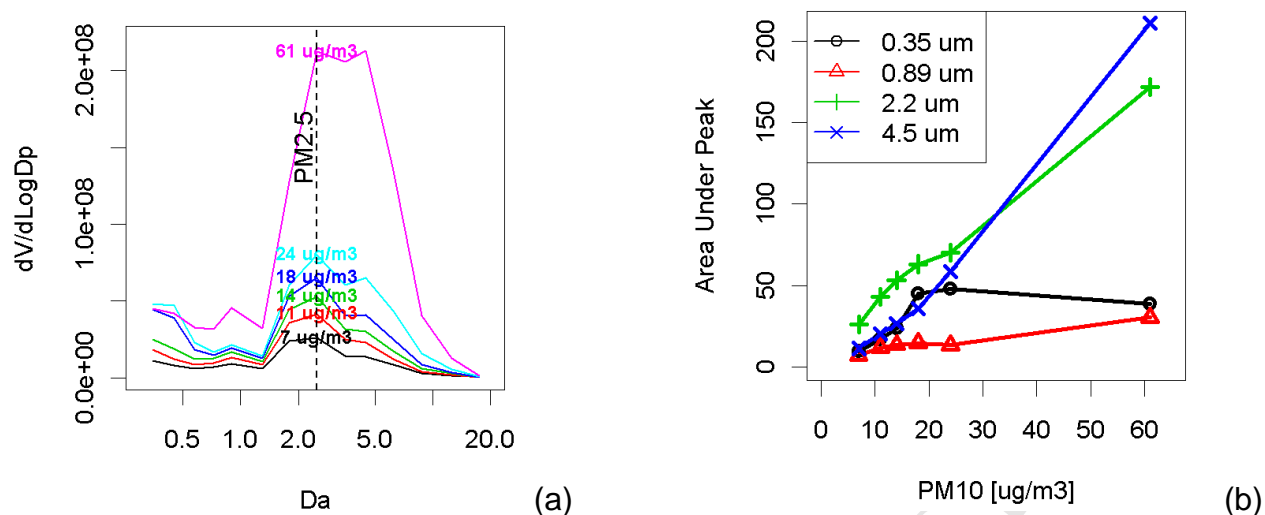


Figure 10. (a) Relationship between area under the curves to measured mean PM₁₀; (b) same data plotted for individual modes within the Grimm size distribution data. Two largest modes with modal diameters at 2.2 and 4.5 μm have the highest correlation with PM₁₀ and have been associated with an FeP particle type from Hot and Cold Mills by Dall'Osto et al. (2008b). [units: dV/dLogDp - $\mu\text{m}^3/\text{cm}^3$].

993
994

Identification of Specific Sources of Airborne Particles emitted from within a Complex Industrial (Steelworks) Site

D.C.S. Beddows and Roy M. Harrison

HIGHLIGHTS

- Contributions of a steelworks to PM mass are assessed
- Directional analysis identifies slag handling as a major source
- Wind-driven resuspension generates coarse particles
- Chemical composition at upwind and downwind sites defines sources
- Correlation of PM with SO₂ is due to a process emission source